Report

R-19-08

January 2019

Hydrogeochemical conditions during periods with glacial and periglacial climate conditions

Report for the safety evaluation SE-SFL

María J. Gimeno

Luis F. Auqué

Javier B. Gómez

SVENSK KÄRNBRÄNSLEHANTERING AB

SWEDISH NUCLEAR FUEL
AND WASTE MANAGEMENT CO

Box 3091, SE-169 03 Solna
Phone +46 8 459 84 00
skb.se

SVENSK KÄRNBRÄNSLEHANTERING

ISSN 1402-3091
SKB R-19-08
ID 1550104

January 2019

Hydrogeochemical conditions during periods with glacial and periglacial climate conditions

Report for the safety evaluation SE-SFL

María J. Gimeno, Luis F. Auqué, Javier B. Gómez
University of Zaragoza

Summary

The present work is part of the SFL safety evaluation and deals with the chemical composition of groundwater in the rock volume surrounding the repository.

In order to provide input to the site selection process for SFL the safety evaluation aims at evaluating the proposed repository concept (Elfwing et al. 2013) at a representative site in Sweden. The evaluation will be performed with existing data from SKB's site investigation programs for the nuclear fuel repository in Laxemar and Forsmark and from less extensive investigations performed at a few other sites. In the present work, geological data from the Laxemar area is used to represent typical Swedish bedrock.

During the 1 million year analysis period for post-closure safety for SFL, climate at a repository site in Sweden is expected to vary within the range represented by the temperate, periglacial and glacial climate domains. These variations, and the associated variations in hydraulic conditions, are expected to alter the chemical composition of groundwater in the rock volume surrounding the repository. The geochemical evolution during a period of temperate climate conditions was described for SE-SFL by Joyce et al. (2019).

This report describes an evaluation of the geochemical evolution during periods of periglacial and glacial climate conditions for two alternative repository depths (500 and 700 m). During such periods, the repository will be under permafrost or under an ice sheet and, therefore, the groundwater chemistry is expected to change by the infiltration of glacial melt waters, and by the upconing of deep saline groundwater. Then, after the retreat of the ice sheet, isostatic depression will set the ground surface at the repository site below a water body, either a brackish or a meltwater lake, for a period of time.

The present evaluation is based on two calculation cases defined by Vidstrand et al. (2010), who simulated groundwater flow in Laxemar:

- The simulation of "Glacial climate conditions without permafrost" which describes a glacial cycle with a succession of ice sheet advance over unfrozen ground towards the repository site, a period of complete ice sheet coverage at the repository site, and ice sheet retreat with submerged ground conditions in front of the ice sheet margin.
- The simulation of "Glacial climate conditions with permafrost" which describes ice sheet advance with permafrost in front of the ice sheet margin.

The groundwater salinity distributions in the rock volume surrounding the repository from Vidstrand et al. (2010) are used as input to a geochemical mixing and reaction model. Thus, the calculated geochemistry is in agreement with the salinity determined by the geohydrological model. Discussions of the results are focused on the Eh, the pH and the concentration of some solutes, as these may influence the chemical stability of the repository and radionuclide transport.

The results obtained with the performed simulations indicate that: 1) the salinities decrease within the repository volume at both studied depths during the simulated glacial cycle, affecting some of the chemical parameters, 2) the computed pH remains below 10 (between 6.5 and 9.6) during the simulated glacial cycle, and 3) the Eh shows a wide variability (between −350 and −150 mV for the mean values) but always with reducing values.

Sammanfattning

Denna rapport är en del av säkerhetsvärderingen SE-SFL och behandlar grundvattnets kemiska sammansättning i bergvolymen kring förvaret.

Säkerhetsvärderingen syftar till att kunna ge input till platsvalprocessen för SFL, genom att analysera det föreslagna förvarets koncept (Elfwing et al. 2013) på en representativ plats i Sverige. Utvärderingen kommer att utföras med befintliga data från SKB:s platsundersökningar för kärnbränsleförvaret i Laxemar och Forsmark och från mindre omfattande undersökningar utförda på några andra platser. I detta arbete används geologiska data från Laxemar-området för att representera typisk svensk berggrund.

Under analysperioden för SE-SFL, som varar i 1 miljoner år, förväntas klimatet på en förvaringsplats i Sverige variera inom det spann som representeras av tempererade, periglaciala och glaciala klimattyper. Dessa variationer och tillhörande variationer i hydrauliska förhållanden förväntas förändra grundvattnets kemiska sammansättning i bergvolymen kring förvaret. Den geokemiska utvecklingen under en period av tempererade klimatförhållanden beskrevs för SE-SFL av Joyce et al. (2019).

Denna rapport beskriver en utvärdering av den geokemiska utvecklingen under periglaciala- och glaciala perioder för två alternativa djup (500 och 700 m). Under sådana perioder kommer förvaret att vara under permafrost eller under en inlandsis och därför förväntas grundvattenkemin förändras genom infiltrering av smältvatten och genom uppträngning av djupa salta grundvatten. Efter inlandsisens reträtt kommer den isostatiska fördjupningen att resultera i att markytan på förvarets plats täcks under en period av vatten, antingen en bräckt- eller smältvattensjö.

Den föreliggande utvärderingen bygger på två beräkningsfall definierade av Vidstrand et al. (2010), som simulerade grundvattenflödet i Laxemar:

- Simuleringen av ”Glaciala klimatförhållanden utan permafrost” som beskriver en glaciationscykel med en följd av inlandsis som avancerar mot förvaret på ofrusen mark, en period med fullständig inlandsistäckning av förvaret, och inlandsisens reträtt med marken under havsnivån framför iskanten.
- Simuleringen av ”Glaciala klimatförhållanden med permafrost”, som beskriver inlandsisens avancemang med permafrost förhållanden framför iskanten.

Grundvattnets saltfördelning i bergvolymen som omger förvaret från Vidstrand et al. (2010) används som indata till en geokemisk blandnings- och reaktionsmodell. Således är den beräknade geokemin i överensstämmelse med salthalten bestämd av den geohydrologiska modellen. Diskussionen kring resultaten fokuserar på Eh, pH och koncentrationen av vissa lösta ämnen, eftersom dessa kan påverka kemisk stabilitet hos förvaret och radionuklidtransporten.

Resultaten från de utförda simuleringarna indikerar att 1) salthalten minskar i förvarsvolymen vid båda undersökta djupen under den simulerade glaciala cykeln, vilket påverkar några av de kemiska parametrarna, 2) det beräknade pH-värdet förblir under 10 (mellan 6,5 och 9,6) under den simulerade glaciala cykeln och 3) Eh visar en stor variabilitet (mellan −350 och −150 mV för medelvärdena) men är alltid reducerande.

Contents

1 Introduction

1.1 Background

SKB plans to dispose of the long-lived low and intermediate level waste in SFL. The waste comprises operational and decommissioning nuclear waste of the Swedish nuclear power plants, legacy waste from the early research in the Swedish nuclear programmes, and smaller amounts of waste from hospitals, industry and research (Elfwing et al. 2013). In the proposed concept (Elfwing et al. 2013), SFL is as a deep geological repository with two storage vaults:

- one vault for the metallic waste from the nuclear power plants, which is designed with a concrete barrier, and
- one vault for legacy waste from AB SVAFO and Studsvik Nuclear AB, which is designed with a bentonite barrier.

In order to provide input to the site selection process for SFL the safety evaluation aims at evaluating the proposed repository concept at a representative site in Sweden. The evaluation will be performed with existing data from SKB's site investigation programs for the nuclear fuel repository in Laxemar and Forsmark and from less extensive investigations performed at a few other sites. In the present work, geological data from the Laxemar area is used to represent typical Swedish bedrock.

The methodology used for the calculations and the basic structure of this report are the same as the ones presented for the evaluation of the Laxemar site within the SR-Site project (Gimeno et al. 2010).

1.2 Objective

The specific objective of this work is to estimate the hydrogeochemical conditions during periods of periglacial and glacial climate conditions in the rock volume chosen for the safety evaluation SE-SFL and at two different depths (500 and 700 m). The present evaluation is based on two calculation cases defined by Vidstrand et al. (2010), who simulated groundwater flow in Laxemar:

- The simulation of "Glacial climate conditions without permafrost" which describes a glacial cycle with a succession of ice sheet advance over unfrozen ground towards the repository site, a period of complete ice sheet coverage at the repository site, and ice sheet retreat with submerged ground conditions in front of the ice sheet margin.
- The simulation of "Glacial climate conditions with permafrost" which describes ice sheet advance with permafrost in front of the ice sheet margin.

1.3 Approach

The conceptual model on which the geochemical calculation strategies are based, assumes that the chemical characteristics of the Laxemar groundwater are the result of complex mixing events driven by the input of different recharge waters during the palaeogeographic history of the site (Gimeno et al. 2014, Gómez et al. 2014, Laaksoharju et al. 2009). The hydrogeochemical study has confirmed the existence of at least five component waters (reference waters or end members): an old brine (Deep Saline), an old dilute meteoric water (Old meteoric), a glacial melt-water (Glacial), a marine water (ancient Littorina Sea), and a modern meteoric water (Altered Meteoric; Laaksoharju et al. 2009).

Mixing provides a satisfactory interpretation for several of the groundwater components partly because the rates of reaction between the rock and the circulating groundwater are relatively slow and also because there are large differences in concentrations between the mixing waters. Under such circumstances, the relative effects of water-rock interactions on the concentrations of the main groundwater components are small when compared with the large effects caused by mixing. There are, however, important parameters mainly controlled by equilibrium reactions (homogeneous and heterogeneous) and these must be taken into account, although even in that case, the intensity of water-rock interactions depends on salinity and, therefore, on mixing proportions. Moreover, mixing produces non-linear effects on the thermodynamic activities of the species controlling the water-mineral reactions (e.g. through the ionic activity product) and controls the direction (precipitation or dissolution) and extent of most subsequent heterogeneous reactions in the system (see Gimeno et al. 2009, pp 133–137 and references therein). Therefore, the hydrogeological results are a necessary input for the geochemical calculation.

A numerical methodology, developed and used in the previous SR-Can and SR-Site assessments (Auqué et al. 2006, Gimeno et al. 2010, respectively), has been applied here (with minor technical updates).

The strategy to evaluate the groundwater compositions consists of using the results from the hydrological flow models (Vidstrand et al. 2010) as input to the mixing and reaction models. The hydrogeological model only provides the salinity for each point in the discretised volume of the whole area (and for every stage of the glacial cycle) and, based on the understanding of the palaeohydrogeological history of the sites (which assumes the presence of different water mixing events due to the input of different reference waters over the time), this salinity is transformed in mass fractions of three reference waters: Deep Saline, Altered Meteoric and Glacial. From the salinity alone, the proportions of Littorina and Old Meteoric reference waters may not be obtained, and the proportion of these reference waters is therefore included in the proportions of Deep Saline and Altered Meteoric, respectively. These data are then used as mixing proportions of the end member waters and knowing the chemical composition of these three reference waters, the final groundwater compositions is modelled through mixing calculations and mineral dissolution/precipitation reactions using PHREEQC (Parkhurst and Appelo 2013). A summary of the methodology used here explaining the main modifications and updates is presented in Chapter 2.

The input data used in the hydrogeochemical calculations are:

- Groundwater salinity, as a function of time and space, from the hydrogeological model simulations (Vidstrand et al. 2010). Note that the fractions of reference waters were not calculated by the hydrogeological model.
- The chemical composition of the three reference waters: “Deep Saline”, “Altered Meteoric” and “Glacial”.
- The reactions between aqueous species and mineral equilibria.

As in previous calculations (SR-Site; Gimeno et al. 2010), the most relevant data needed here are the geological structure of the site, the hydrogeological data and associated conceptual assumptions, the hydrogeochemical and mineralogical information from the Laxemar site descriptive model and the thermodynamic data used in the geochemical calculations.

2 Method for the geochemical calculations

The methodology used for these calculations is the same as the one used for the SR-Site geochemical calculations in Forsmark and Laxemar (Salas et al. 2010, Gimeno et al. 2010) and a thourogh explanation can be found in the corresponding reports. Here we will only present the basic aspects of the calculation process and the modifications and improvements performed to adapt the tools to the rock volume chosen for the safety evaluation SE-SFL area and to the updates of the geochemical code PHREEQC (Parkhurst and Appelo 2013).

The specific calculation process followed for these calculations is summarised in Figure 2-1. From the hydrogeological model results (expressed as estimated salinity in all the discretised points in the studied rock volume) to the output files obtained by PHREEQC, the programs used here are the same as those used for SR-Site. However, there are two main differences with respect to the procedure followed there. The first one is that the entire process has been automatised by the use of two scripts that are explained in Appendix 1. The second difference is that in the new version, the program developed to obtain the selected data from the PHREEQC output file, is not necessary as now the own PHREEQC input files are created to contain the necessary instructions to make the program to create its own selected output file. The file containing these instructions is also described in Appendix 1 (A1.5.2).

The evolution of the groundwater composition has been simulated based on two calculation cases defined by Vidstrand et al. (2010), who simulated groundwater flow in Laxemar:

- The simulation of "Glacial climate conditions without permafrost" which describes a glacial cycle with a succession of ice sheet advance over unfrozen ground towards the repository site, a period of complete ice sheet coverage at the repository site, and ice sheet retreat with submerged ground conditions in front of the ice sheet margin.
- The simulation of "Glacial climate conditions with permafrost" which describes ice sheet advance with permafrost in front of the ice sheet margin.

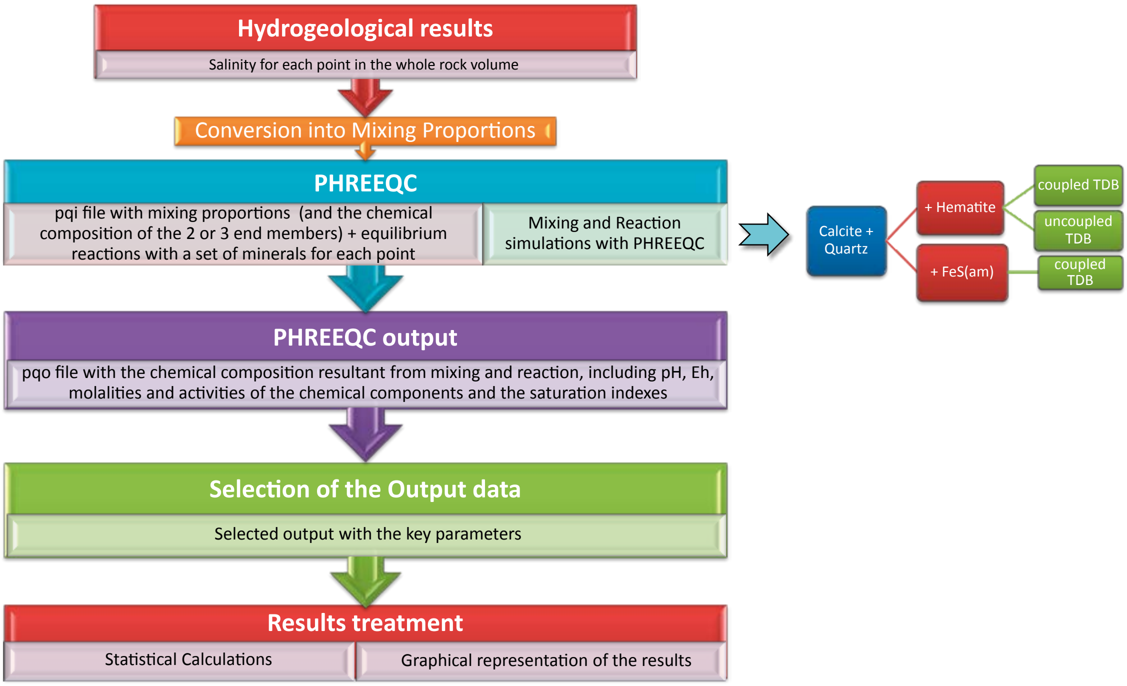

Figure 2-1. *Steps followed for the geochemical simulations (modified from Gimeno et al. 2010).*

The glacial cycle comprises approximately 13 000 years between the first ice front passage until the site, once again, becomes ice free, however submerged beneath a fresh water lake. The different stages (i.e. ice margin positions) and hydrological cases considered in the calculations can be found in Vidstrand et al. (2010; see, for example, Figure 1-5 and 5-4) and they are summarised in Table 2-1 (see also Gimeno et al. 2010 for a more detailed explanation). They include the advance of the ice front to different locations (Ice 0a to Ice Va, when the ice covers the entire model domain) and then its retreat to some of the previously considered positions ending when the area is ice-free again after a full glacial cycle (Ice 0r). The geochemical calculations performed here have been carried out with the *hydrological Base Case* (see Selroos and Follin 2010, Vidstrand et al. 2010) where the ice front has a frontal angle of 45 degrees, and moves over an unfrozen surface in a NW-SE direction and with the variant case where permafrost develops during the glacial period (Table 2-1). In the variant case where permafrost develops during the glacial period, the initial stage represents frozen conditions (periglacial period) with "taliks" before the ice advance, and the progressive advance of the ice (Ice Ia to Ice IVa) with permafrost development to 2 km under the ice margin and with the presence of taliks.

The volumes chosen for the SE-SFL simulations have been:

- The rock volume at 500 m depth chosen for the safety evaluation SE-SFL: the volume included in the domain inside the following coordinates (in km): [1 546.8, 6 367.0, −0.5]; [1 546.8, 6 367.5, −0.5]; [1 547.2, 6 367.5, −0.5]; and [1 547.2, 6 367.0, −0.5] with a thickness between −528 and −464 m depth. This volume contains 624 grid points.
- An alternative rock volume at 700 m depth: the volume included in the domain inside the following coordinates (in km): [1 546.8, 6 367.0, −0.7]; [1 546.8, 6 367.5, −0.7]; [1 547.2, 6 367.5, −0.7]; and [1 547.2, 6 367.0, −0.7]) with a thickness between −672 and −736 m depth. This volume contains 96 grid points.
- A vertical plane has also been selected. This plane is approximately parallel to the shoreline (in km, NW: 1 544.5/6 370; SE: 1 551.5 m/6 363.025) and parallel to the ice front movement, through boreholes KLX13A, KLX18A, KLX12A and KLX05, with 20 372 grid points.

Once the data subsets for the SFL volume or the vertical plane are extracted, the calculations start with the transformation of the salinities given by the hydrogeologists, into mixing proportions (of Deep Saline, Altered Meteoric and Glacial reference waters) for each time slice (Figure 2-1). For the initial stage (Ice 0) salinity is used to obtain mixing proportions of only two components, Deep Saline and Altered Meteoric (see Gimeno et al. 2010 for a detailed explanation). For the subsequent stages (with the advancement and retreat of the glacier) the proportion of a third mixing end-member is calculated from the change of salinity at any point in the rock volume (a newly incoming glacial melt-water, when there is a dilution, or the upconing of deeper and more saline waters when the salinity increases), changing the proportions of the other two reference waters correspondingly (a detailed explanation of the procedure and a discusion about its uncertainties and limitations can be found in Gimeno et al. 2010).

After the mixing proportions have been obtained from the salinities, PHREEQC input files are created to perform the mixing and reaction simulations equilibrating each mixed water with a set of minerals (Figure 2-2). The selected phases are present in the system as rock-forming minerals and fracture fillings and have fast kinetics for the simulated time intervals. All the geochemical simulations performed here include mixing and equilibrium reactions with calcite, quartz, and a redox mineral that changes depending on the geochemical case (see also Gimeno et al. 2010):

- Geochemical case 1: equilibrium with haematite using the coupled thermodynamic data base (see below).
- Geochemical case 2: equilibrium with FeS(am) using the coupled thermodynamic data base.
- Geochimical case 3: equilibrium with haematite using the uncoupled thermodynamic data base.

The objective of using these three different geochemical cases is to try to capture the conceptual uncertainties in the knowledge of the redox system at the site: equilibrium with haematite implies a situation where the redox state is not affected by sulfate-reducing bacteria, while equilibrium with FeS(am) characterises a situation with significant activity of sulfate-reducing bacteria (Gimeno et al. 2010, Salas et al. 2010). The third case considers the possible control of Eh by the iron system and the $Fe(OH)_3/Fe^{2+}$ redox pair (mantaining homogeneous redox disequilibrium) and, therefore, using the un-coupled thermodynamic database; see below).

Table 2-1. Cases and stages for which geochemical simulations over the glacial cycle have been performed (Vidstrand et al. 2010), giving the name of the hydrogeological file, the position of the sea level and the ice front location, movement, angle and coordinates. The initial state (at time = 0) and the model network are the same in all cases.

File name	Special Case	Sea Level	Ice movement	Ice Front Angle	Climate domain/ Ice Front location	Ice Front Location Coordinates				Local Darcy Tools	
						Local Darcy Tools		RT90		Origo (RT90)	
						X(km)	Y(km)	X(km)	Y(km)	X0(km)	Y0(km)
GLACIAL CYCLE WITHOUT PERMAFROST											
Chem_delivery_Laxemar_0.txt		0	–		temperate	−31.3	0	1 507.7	6 360.0	1 539	6 360
Chem_delivery_Laxemar_I.txt		0	advance	−45	Ice I	1.1	0	1 540.1	6 360.0	1 539	6 360
Chem_delivery_Laxemar_II.txt		0	advance	−45	Ice II	3.2	0	1 542.2	6 360.0	1 539	6 360
Chem_delivery_Laxemar_III.txt		0	advance	−45	Ice III	4.4	0	1 543.4	6 360.0	1 539	6 360
Chem_delivery_Laxemar_IV.txt		0	advance	−45	Ice IV	27.8	0	1 566.8	6 360.0	1 539	6 360
xyzpss_lax_BC_IFLVa.txt		100	advance	−45	Ice Va						
xyzpss_IPV2.txt		100	retreat	−45	Ice Vr						
Chem_delivery_Laxemar_IVr.txt		100	retreat	−45	Ice IV	27.8	0	1 566.8	6 360.0	1 539	6 360
Chem_delivery_Laxemar_IIr.txt		100	retreat	−45	Ice II	4.4	0	1 543.4	6 360.0	1 539	6 360
Chem_delivery_Laxemar_0r.txt		100	–		temperate						
ICE SHEET ADVANCE WITH PERMAFROST											
xyzpss_lax_frozenground_IFL0.txt	Perm_2km	−8	–	–	frozen						
xyzpss_lax_perm_IFLI.txt	Perm_2km	−8	advance	−45	Ice I	1.1	0	1 540.1	6 360.0	1 539	6 360
xyzpss_lax_perm_IFLII.txt	Perm_2km	−8	advance	−45	Ice II	3.2	0	1 542.2	6 360.0	1 539	6 360
xyzpss_lax_perm_IFLIII.txt	Perm_2km	−8	advance	−45	Ice III	4.4	0	1 543.4	6 360.0	1 539	6 360
xyzpss_lax_perm_IFLIV.txt	Perm_2km	−8	advance	−45	Ice IV	27.8	0	1 566.8	6 360.0	1 539	6 360

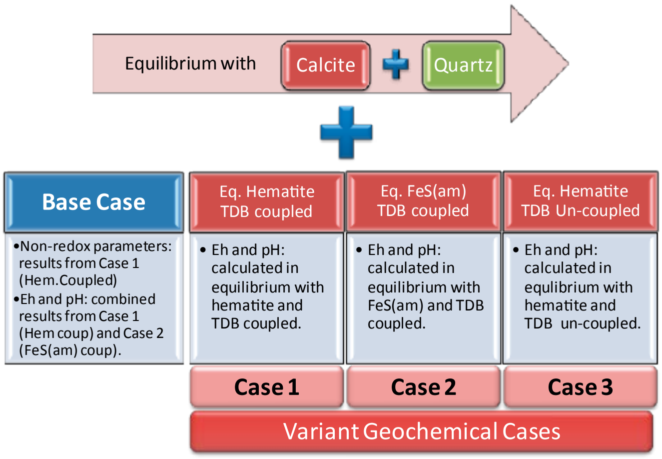

Figure 2-2. *Different geochemical simulations performed for all the periods analysed (modified from Gimeno et al. 2010).*

A Base Case, which includes the results obtained with the variant geochemical Case 1 (equilibration with haematite) for all parameters except for Eh and pH for which, it includes also the results obtained with the variant geochemical Case 2 (equilibration with FeS(am)), is defined.

Directly related to this, two very important aspects to be considered when running PHREEQC for these simulations are: the thermodynamic data base and the composition of the end members. A comprehensive explanation of these key aspects in the geochemical calculations performed for SR-Site in Laxemar can be found in Gimeno et al. (2010) but the main updates are shortly indicated below.

The thermodynamic database used for the geochemical calculations (SKB 2013) is the same as the one used by Joyce et al. (2019) for the modelling of temperate conditions for SE-SFL (SKB-2009_vers-3_SFL-modified_150528.dat), which is basically the one used by Salas et al. (2010) and Gimeno et al. (2010) for the SR-Site calculations with some corrections and updates. For example the following mineral phases have been added:

- Fe(OH)$_3$(hematite_grenthe): $Fe(OH)_3 + 3H^+ = Fe^{3+} + 3H_2O$ (log_k = −1.10)
- FeS(ppt): $FeS + H^+ = Fe^{2+} + HS^-$ (log_k = −3.00)
- Albite: $NaAlSi_3O_8 + 8H_2O = Al(OH)_4^- + 3Si(OH)_4 + Na^+$ (log_k = −19.98)
- K-Feldspar: $KAlSi_3O_8 + 8H_2O = Al(OH)_4^- + 3Si(OH)_4 + K^+$ (log_k = −22.62)
- Kaolinite_Grimaud: $Al_2Si_2O_5(OH)_4 + 7H_2O = 2Al(OH)_4^- + 2H^+ + 2Si(OH)_4$ (log_k = −37.3)

The reasons behind the selection of these phases and their equilibrium constants are detailed in Auqué et al. (2006) and Gimeno et al. (2009). Additionally, a modified version of the thermodynamic database (named the "uncoupled" database) was implemented to consider the effects of the homogeneous redox disequilibria. Further details on the meaning and procedure followed to implement this modification are explained in Auqué et al. (2006) and Gimeno et al. (2010).

With respect to the original chemical composition of the reference waters, the ones used here are those shown in Table F-1 by Joyce et al. (2010) (thorough descriptions and discussions about why and how these compositions have been estimated can be found in Gimeno et al. 2008, 2009, 2010). However, as there are some unknown fundamental parameters for some of these reference waters (pH, Eh, concentration of Al, Fe, or S(−II)), their values have been obtained assuming a series of mineral equilibrium reactions thought to be controlling these variables (e.g. with calcite, quartz, haematite and/or Fe(II)-monosulfides; see Gimeno et al. 2010 for further details). Additionally, all equilibrated reference waters were charge balanced by adjusting the chloride concentration. The final chemical composition of the end members as they have been used in the geochemical modelling performed for SFL with the coupled and uncoupled thermodynamic data base, is shown in Appendix 1 (Section A1.5.3).

Once the PHREEQC output files have been obtained, the PHREEQC program extracts the desired information (selected by the user with the SELECTED OUTPUT option) contained in them in a tabulated form with the extracted information in columns and the grid points in rows. The results obtained include the detailed chemical compositions of the groundwater at each point.

3 Results and discussion

As indicated in Section 1.2, the main aim of the work presented here is to calculate and describe the chemical composition of the groundwater in the rock volume in Laxemar chosen for the safety evaluation SE-SFL at 500 and 700 m depth. The evolution stages considered here cover the time span just after the temperate period, that is, a glacial cycle (including the permafrost and the glacial stages) starting at the end of the temperate period and finishing with the stage immediately after the retreat of the ice sheet which is assumed to be similar to the stage at the beginning of the cycle (or at the end of the temperate period).

In general terms, the infiltration of meteoric water, the displacement of the Baltic shore line, etc. will influence the hydrology of the site during the initial temperate period after closure. These phenomena will induce changes in the geochemical composition of groundwater around the repository. According to the reconstruction of the Weichselian glacial cycle (SKB 2006), which was used as a reference evolution in SR-Can (SKB 2006) and SR-Site (SKB 2011), the Laxemar site was covered by inland ice during a few periods with a total duration of less than 30 000 years (out of a total of 120 000 years). Further, permafrost did not occur over a continuous period of time, but rather thawing occured between more or less short periods of permafrost. Some of these permafrost periods coincided with the time when the site was covered by an ice sheet, with “basal frozen” conditions, that is, assuming that the ground was frozen to some extent under the ice sheet.

This chapter presents the results obtained for the evolution of the groundwater during the glacial and periglacial periods with respect to the main geochemical parameters. The statistical results within the rock volume chosen for the safety evaluation SE-SFL at the two studied depths are graphically presented as box and whisker plots and the statistical results corresponding to the Base Case are included in the form of tables in Appendix 2. The results about the Eh evolution are different for the different simulated geochemical cases and, therefore, all of them are described and their corresponding plots are also shown.

3.1 Evolution of the salinity

This section describes the evolution of the salinity (represented by the total dissolved solids, TDS) over the simulated periods. The hydrogeological results indicate a general decrease in the salinity values as the glacial period evolves and the same is indicated by the TDS calculated here through the geochemical modelling considering mixing and reaction (Figure 3-1). This decrease is also evident when considering the presence of permafrost and at the two repository depths studied (500 and 700 m) although the range of values is different in the different situations.

The salinity distribution simulated for the Stage Ice 0a of the glacial period represents a similar situation as the last time slice in the temperate period (see Joyce et al. 2019). The ice sheet totally covers the SFL repository area since the beginning of the simulated period (stages Ice Ia to Ice Va; Figure 3-1, panels a and c) and, therefore, after the first simulation stage the salinity decreases in all the volume due to the constant infiltration of glacial melt waters. Moreover, as the repository volume is located behind the ice front, it is not affected by the expected upconing effect that will happen there. This is clearly seen in Figure 3-1e, where the vertical section (NW-SE) is represented and the two SE-SFL repository volumes, at 500 m and 700 m, are shown. The position of the two volumes is already behind the ice front location at the first stage of ice advance (Ice 1a) and, as the TDS distribution shows in Figure 3-1e, they are not affected by the upconing effect created just in front of the ice.

After 11 000 years the glacier begins to retreat (stages Ice Vr, IVr and IIr; Figures 3-1a and c) and the salinity keeps decreasing until the end of the glacial cycle (stage Ice 0r) when there is a new increase in the salinity values at the two studied depths. This last stage will be the result of the retreat of the ice sheet and the isostatic depression that will place the ground surface at the repository site below the Baltic Sea surface level for a while, creating a situation similar to that at the end of the temperate period. A relatively fast turnover of groundwater, where glacial melt water is replaced by a succession of waters penetrating from the surface, is expected during this period: the equivalent to the Littorina sea gradually evolving into the equivalent to the present-day Baltic Sea.

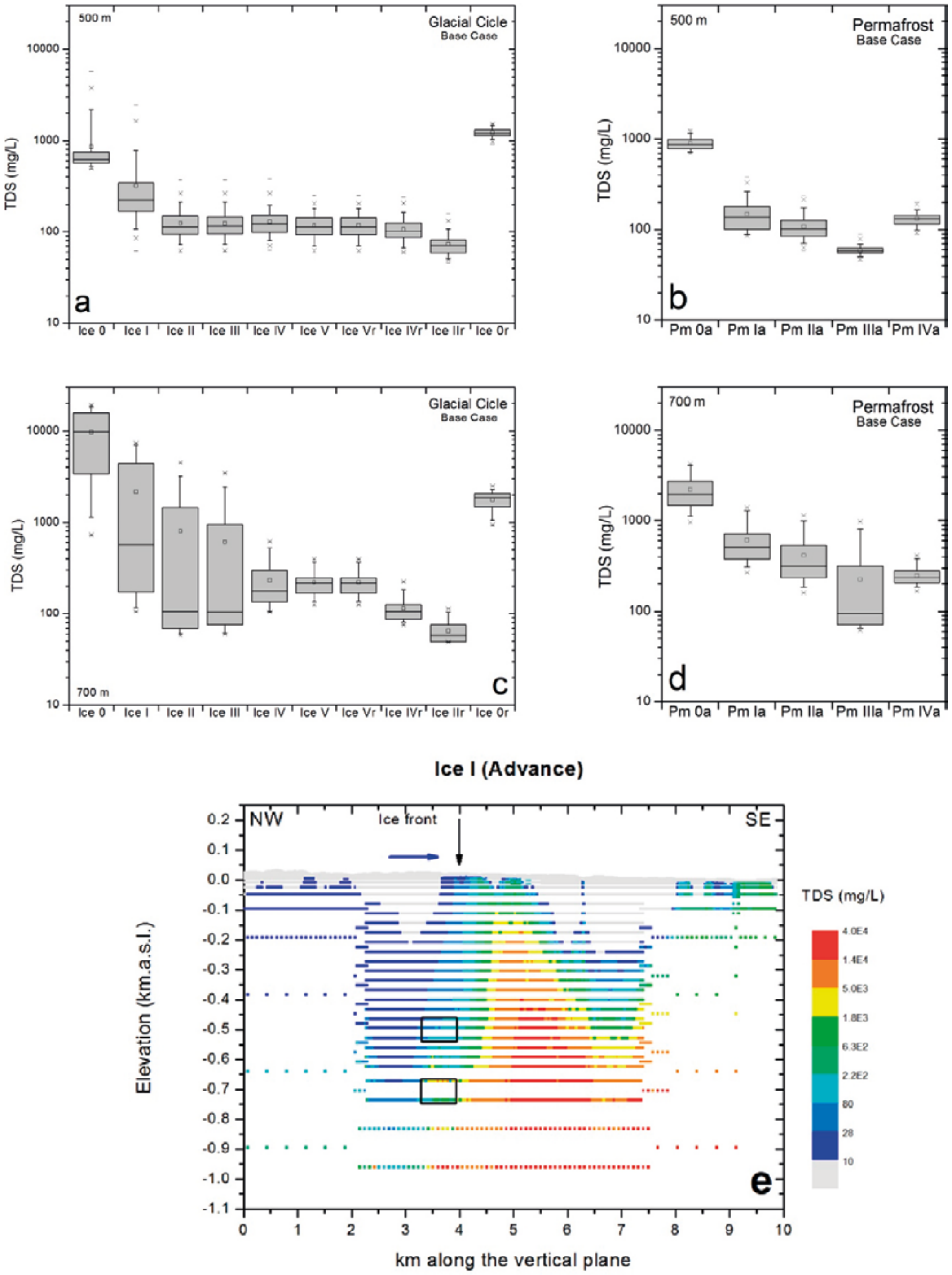

Figure 3-1. *Box-and-whisker plots showing the results obtained for the Base Case for the predicted statistical distribution of TDS (in mg/L) for the different glacial stages when considering an ice-sheet advancing over unfrozen ground (a, c) and when considering an ice-sheet advancing over frozen ground (permafrost) (b, d) for groundwater within the SE-SFL repository volume at Laxemar at 500 m (a and b) and at 700 m (c and d). The statistical measures plotted here and in all the following box and whiskers plots, are the median (horizontal line inside the grey box), the 25th and 75th percentiles (bottom and top of the box), the mean (square), the 5th and 95th percentiles ("whiskers"), the 1st and 99th percentile (crosses) and the maximum and the minimum values (horizontal bars). Panel e shows the distribution of TDS in the vertical plane and the position of the two repository volumes just behind the ice front and the upconing effect.*

As expected, the salinity values are higher at 700 m depth and with a wider range of variation for almost all the glacial stages, probably due to the fact that the melt waters arrive more slowly at this depth and very different salinities will coexist during longer periods. At this depth the decrease in salinity is also more marked than at 500 m (Figure 3-1a and c) mainly from the stage 0a to the stage IIIa, then it tends to stabilise in both cases. At the end of the glacial cycle, the salinity values increase at both depths, but at 500 m the values are even higher than at the beginning of the cycle, while at 700 m, the salinity is almost one order of magnitude lower than at the beginning.

The results obtained for the simulated periglacial condition during the first stages of the evolution (Pm 0a to Pm IVa; Figure 3-1b and d) predict, for the two depths, lower salinities in the repository volume than when permafrost is not considered. Moreover, there is a slight increase in salinity at the stage Pm IVa at both depths (again more marked at 500 m) that is not shown when the glacier advances over an unfrozen soil. The main difference between the results obtained for the two studied depths in the periglacial variant, is that the decrease in salinity is more progressive at 700 m and with a broader range of values. Another important difference can be seen at the initial stage. At 500 m depth, the initial salinity values are slightly higher than the ones obtained without a frozen soil (panel a), while at 700 m depth, the situation is the opposite.

Finally, after these first stages with the frozen soil, the rest of the evolution is expected to be the same as the one observed when permafrost is not considered.

3.2 pH values and total inorganic carbon concentrations

Calculations indicate that the onset of glacial conditions may result in a general increase of pH values (Figure 3-2), an effect which is commonly observed in this type of glacial groundwaters (see Gimeno et al. 2010). The pH obtained for almost all the glacial period (with or without permafrost) and for the two considered depths (500 and 700 m) is fairly high.

The main difference at the two depths is, as for the salinity, that the range of variation is larger at 700 m, starting with lower values around 6.7 and reaching the maximum pH values at around 9.5 just before the end of the glacial cycle (Ice IIr) (at 500 m, the first values are around 7.5 and they increase up to around 9.2 at the Stage Ice IIr). The range of pH values at 700 m during the first evolution stages (Ice 0 to Ice III) is very wide (more than 1 pH unit), but then it tends to stabilise at a value around 9.0 for the whole volume, just slightly higher than at 500 m. These stable values persist during the time the glacial front is far (stages Ice IVa to Ice IVr). Then the pH value in the final stage at the end of the glacial cycle is also higher at 700 m (around 8.6) than at 500 m (around 8).

In the case of the evolution considering the frozen ground (Figure 3-2 b and d), the pH values at 500 m are, in general, higher than the values when the permafrost is not considered and the highest ascent happens at the first stage of the evolution (Pm Ia). At 700 m, however, the pH values obtained for the periglacial case are slightly lower than when the permafrost is not considered and also lower than the values at 500 m depth.

Although the results shown here correspond to the Base Case, which includes the values obtained when equilibrating the waters with haematites (Case 1) and with the amorphous monosulfide (Case 2) (in both cases with the coupled thermodynamic database), the calculated pH values are the same irrespective of the geochemical variant case used and, as a summary, in all the cases the pH is predicted to remain lower than 10.

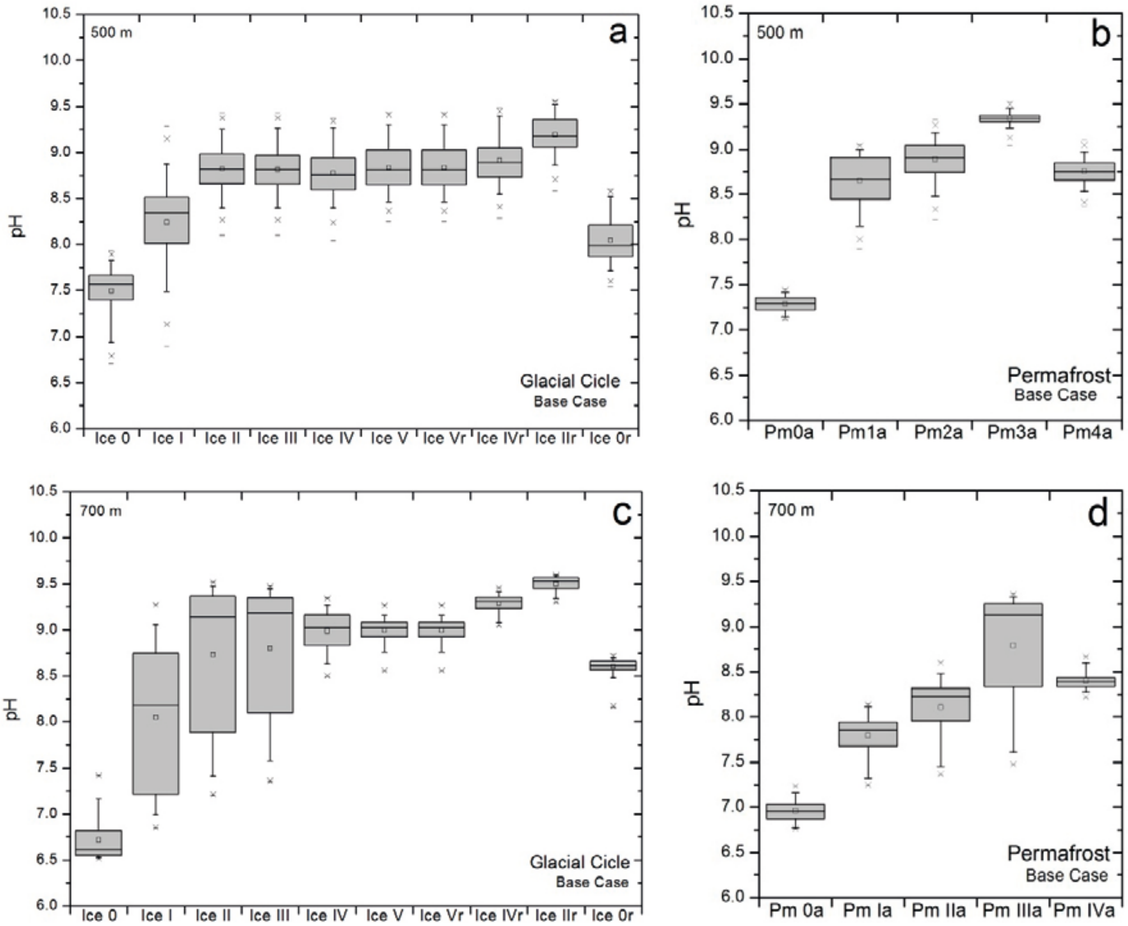

Figure 3-2. *Box-and-whisker plot showing the statistical distribution of the pH (in standard units) calculated when considering an ice-sheet advancing over unfrozen ground (a, c) and when considering an ice-sheet advancing over frozen ground (permafrost) (b, d) for the groundwater located within the SE-SFL repository volume at Laxemar at 500 m (a, b) and 700 m (c, d). See the caption of Figure 3-1 for the statistical meaning of the different symbols.*

As shown in Figure 3-3, log pCO_2 behaves exactly opposite to pH with very low values in all the cases (lower than atmosphere) except at the beginning of the glacial cycle (stage 0a) with the highest values at 700 m depth and also when considering the frozen ground (Figure 3-3 b and d).

With respect to the total inorganic carbon content, the evolution shows a progressive decrease during the glacial period (Figure 3-4) that continues even at the end of the cycle. The decrease is about one order of magnitude in the four different situations considered here and the bigger variation is shown at 700 m depth with no frozen soil (Figure 3-4 c). Only in the last periglacial stage (Pm IVa; Figure 3-4 b, d) there is a slight increase in the carbon values which is parallel to the CO_2 partial pressure and just opposite to pH. As for other parameters, the evolution shows the maximum variation during the first stages 0a to IIIa and then a stable range of values persists for the rest of the evolution until the ice retreat and the glacial cycle ends. The stabilisation of values at 500 m is around 7×10^{-4} mol/kg whilst at 700 m is only 1×10^{-4} mol/kg and with a narrower range.

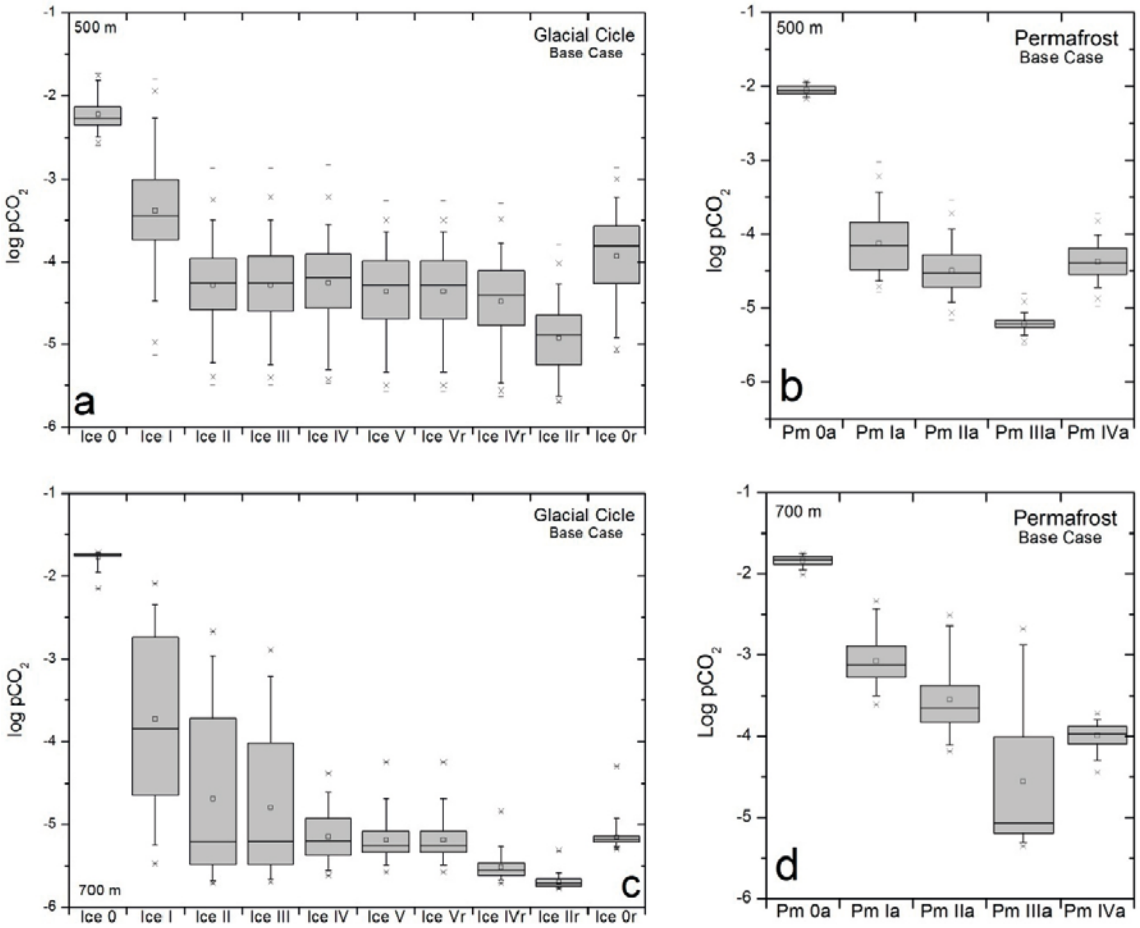

Figure 3-3. *Box-and-whisker plot showing the statistical distribution of the log pCO$_2$ calculated when considering an ice-sheet advancing over unfrozen ground (a, c) and when considering an ice-sheet advancing over frozen ground (permafrost) (b, d) for the groundwater located within the SE-SFL repository volume at Laxemar at 500 m (a, b) and 700 m (c, d). See the caption of Figure 3-1 for the statistical meaning of the different symbols.*

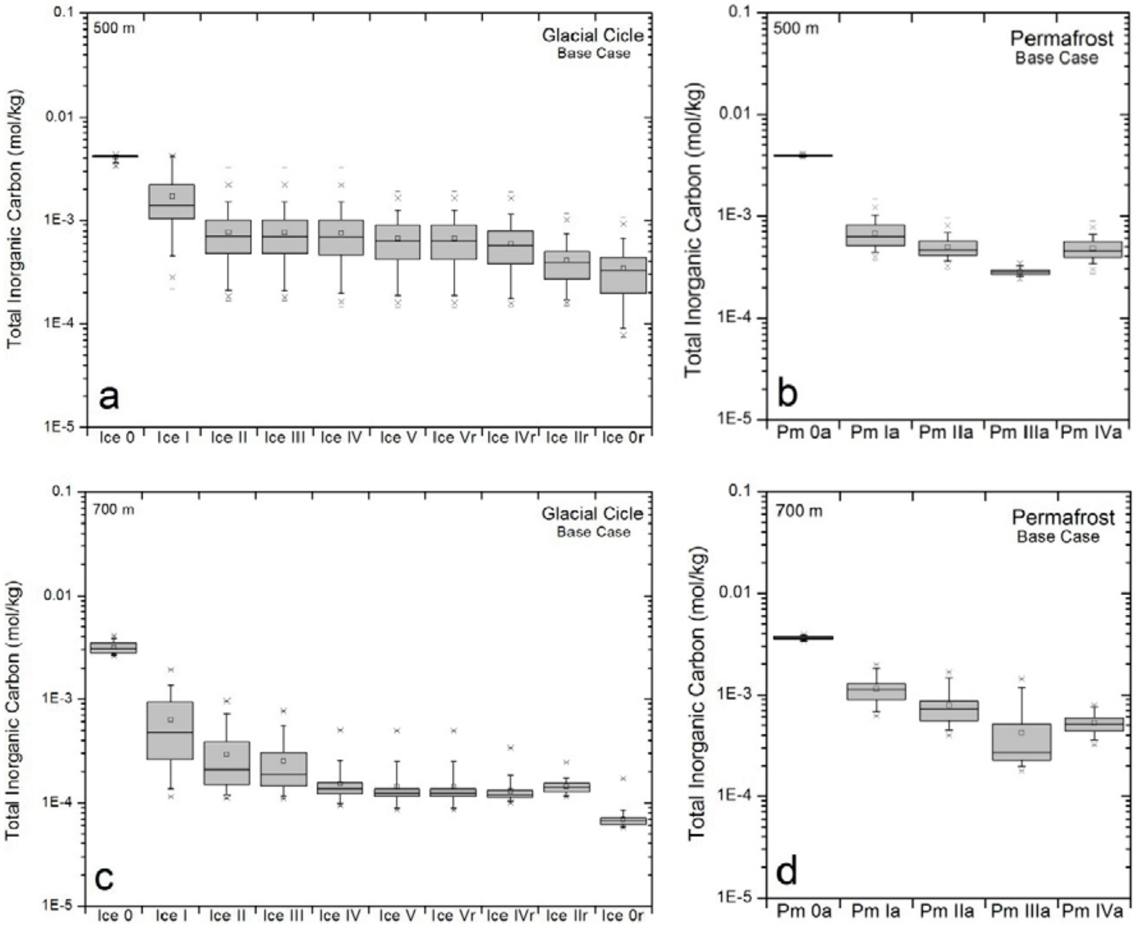

Figure 3-4. *Box-and-whisker plot showing the statistical distribution of the total inorganic carbon content calculated when considering an ice-sheet advancing over unfrozen ground (a, c) and when considering an ice-sheet advancing over frozen ground (permafrost) (b, d) for the groundwater located within the SE-SFL repository volume at Laxemar at 500 m (a, b) and 700 m (c, d). See the caption of Figure 3-1 for the statistical meaning of the different symbols.*

3.3 Redox values: Eh

As indicated previously, the geochemical Base Case for the redox parameters (in this case the Eh) includes not only the results obtained with the geochemical Case 1 (which is the Base case in general for the rest of the geochemical values), but also the results obtained with the geochemical Case 2 (equilibrium with amorphous FeS). However, as the results obtained for the Eh with the two cases are different among them, apart from considering the two sets of results together as a Base Case, they will be presented separately in this section. Additionally, the results obtained with the variant Case 3 (equilibrium with haematite with the uncoupled database; Gimeno et al. 2010) will also be shown and described next.

The evolution of Eh during the glacial period (with or without permafrost), calculated with the Base Case at the two different repository depths (500 m and 700 m) is shown in Figure 3-5. Then, the three separate geochemical variant cases are shown in Figures 3-6 and 3-7 for, the repository at 500 m depth and at 700 m depth respectively.

The results over the whole glacial period with or without perfamorst show a similar evolution trend in all the variant cases (see Figures 3-5 to 3-7). In general, Eh shows a similar trend as other parameters with the initial decrease (from 0a to IIa) towards a more or less stable value for the main stages of the glacial cycle (from IIa to Vr or IVr) and then a final decrease (IIr) before going up at the end of the cycle (stage 0r) back towards the original values before the ice advance.

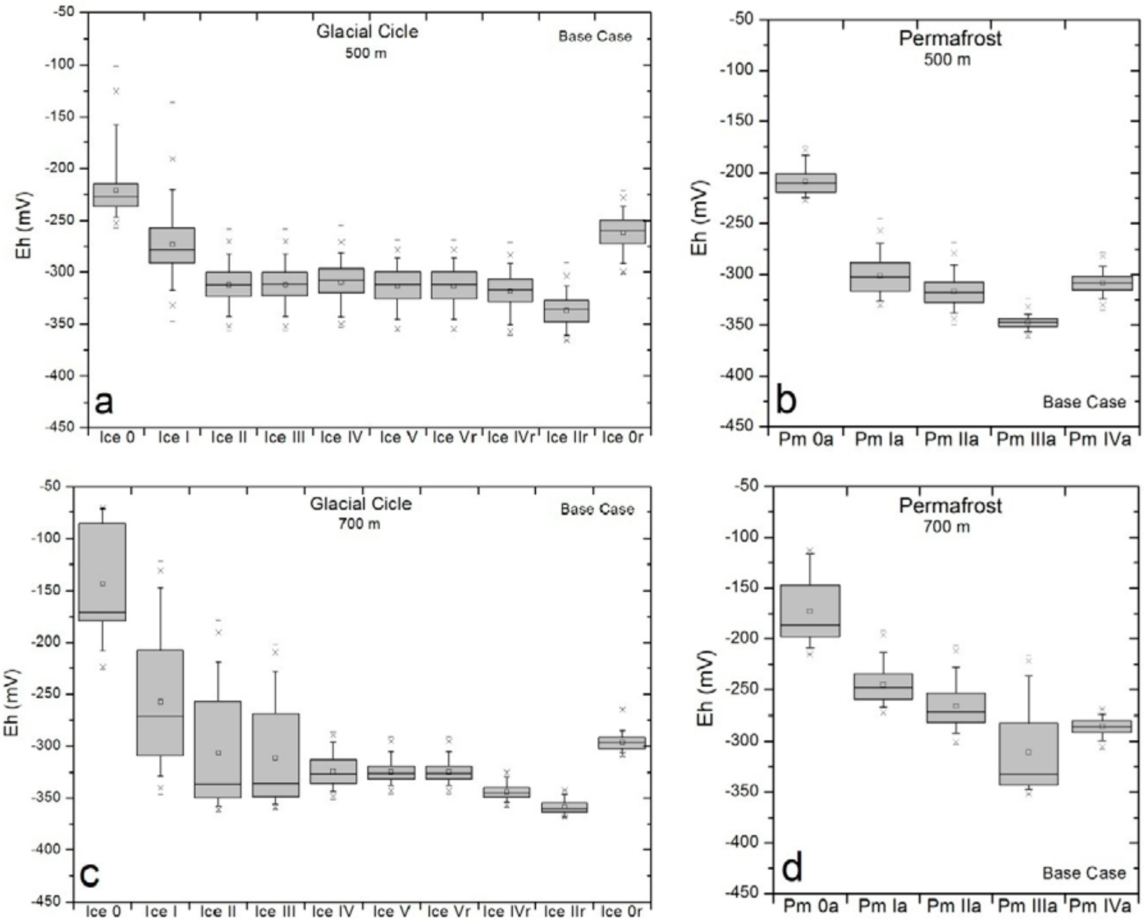

Figure 3-5. Box-and-whisker plot showing the statistical distribution of Eh (mV) obtained for the geochemical Base Case when considering an ice-sheet advancing over unfrozen ground (a, c) and when considering an ice-sheet advancing over frozen ground (permafrost) (b, d) for the groundwater located within the SE-SFL repository volume at Laxemar at 500 m (a, b) and at 700 m depth (c, d). See the caption of Figure 3-1 for the statistical meaning of the different symbols.

The results obtained for the Base Case show less range of variation at 500 m than at 700 m depth. The evolution during the normal glacial cycle at 500 m depth starts with values around −220 mV and then evolves towards lower values around −320 mV to finally increase at the end of the glacial cycle towards value closer to the initial ones (around −250 mV). The evolution at 500 m when considering the frozen ground is very similar to that, although the values at stage 0a are slightly less reducing, and at stage IIIa, slightly more reducing.

The situation at 700 m is slightly more extreme, starting with less reducing values (reaching −75 mV) and with a very variable range of Eh (more than 100 mV) during the first stages (0a to IIIa) and then going down to lower values than the ones reached at 500 m. At the end of the cycle, (Stage 0r), the Eh values at 700 m are around −300 mV, whilst at 500 m depth, they are at around −250 mV. When considering permafrost, the situation is similar with respect to the comparison with the values obained at 500 m.

Comparing the results obtained separately with the 3 geochemical variant cases (Figures 3-6 and 3-7 for the two different depths), it is clear that the Cases 1 and 2 (the ones that together give the Base Case) give very similar values, although Case 2 gives more homogeneous values with a whole range narrower than Case 1. Case 3 always gives the lowest Eh values (50 mV lower than the other 2) for every single stage and irrespective of the presence of permafrost or not.

It is also clear that the differences between Case 1 and 2 are bigger at 700 m depth. The values are higher in Case 1 at the beginning of the cycle (around −100 mV at Ice 0a) and between Ice 0a and Ice IIIa the Eh values decrease almost 200 mV. The range of variation for these first stages is very broad and bigger than what is obtained for Case 2.

Something similar happens when the permafrost is considered, although the initial values are slightly lower (−150 mV). The initial values obtained with Case 2 are around −220 (−200 when Permafrost is considered) and they go down to more or less the same reducing values as with Case 1, keeping the range of variations smaller.

Finally, Case 3 starts exactly the same as Case 1 but then it goes to much lower values (around −400 mV) and with a very broad range of variation. The same can be said for the permaforst compared with the results obtained with the other two variant cases.

In conclusion, for all the glacial periods, with or without frozen ground, the redox potential of the groundwater within the SFL repository domain is expected to be clearly reducing.

Finally, it is important to keep in mind that the methodology used for redox simulations simplify the behaviour of the system by assuming that the imposed equilibria are taking place in the whole volume of rock, which obviously is not true: there are parts of the bedrock where the redox conditions are controlled by the iron system with slight or no influence of sulfate reduction. However, the use of the Base Case, combining the results from variant Cases 1 and 2, gives a practical range of values to be used for the assessment of post-closure safety as they cover almost the whole range of measured Eh values in the present groundwater system in Laxemar.

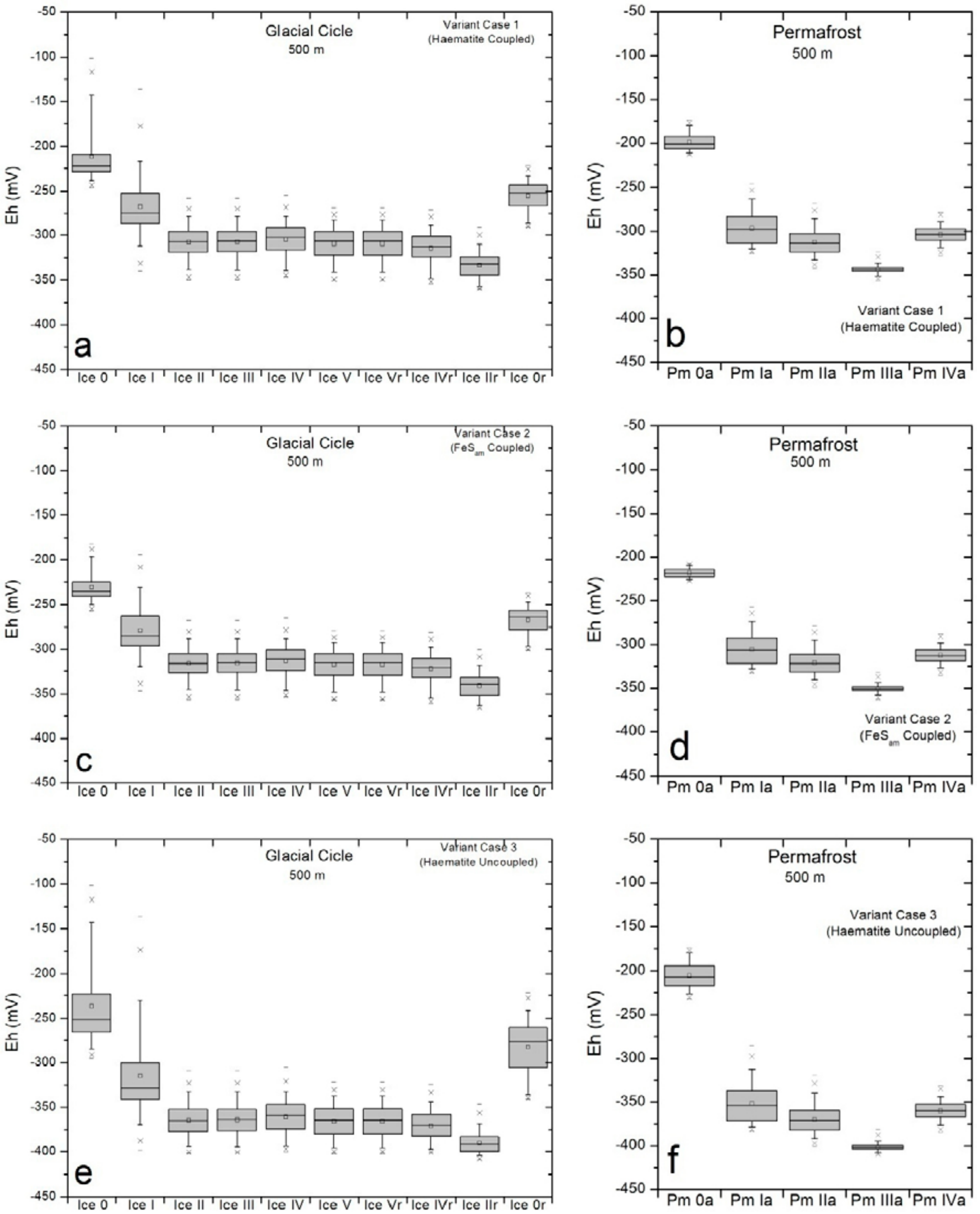

Figure 3-6. Box-and-whisker plot showing the statistical distribution of Eh (mV) obtained for the different geochemical variant cases (Case 1, a and b, Case 2, c and d, and Case 3, e and f) when considering an ice-sheet advancing over unfrozen ground (a, c) and when considering an ice-sheet advancing over frozen ground (permafrost) (b, d) for the groundwater located within the SE-SFL repository volume at Laxemar at 500 m depth. See the caption of Figure 3-1 for the statistical meaning of the different symbols.

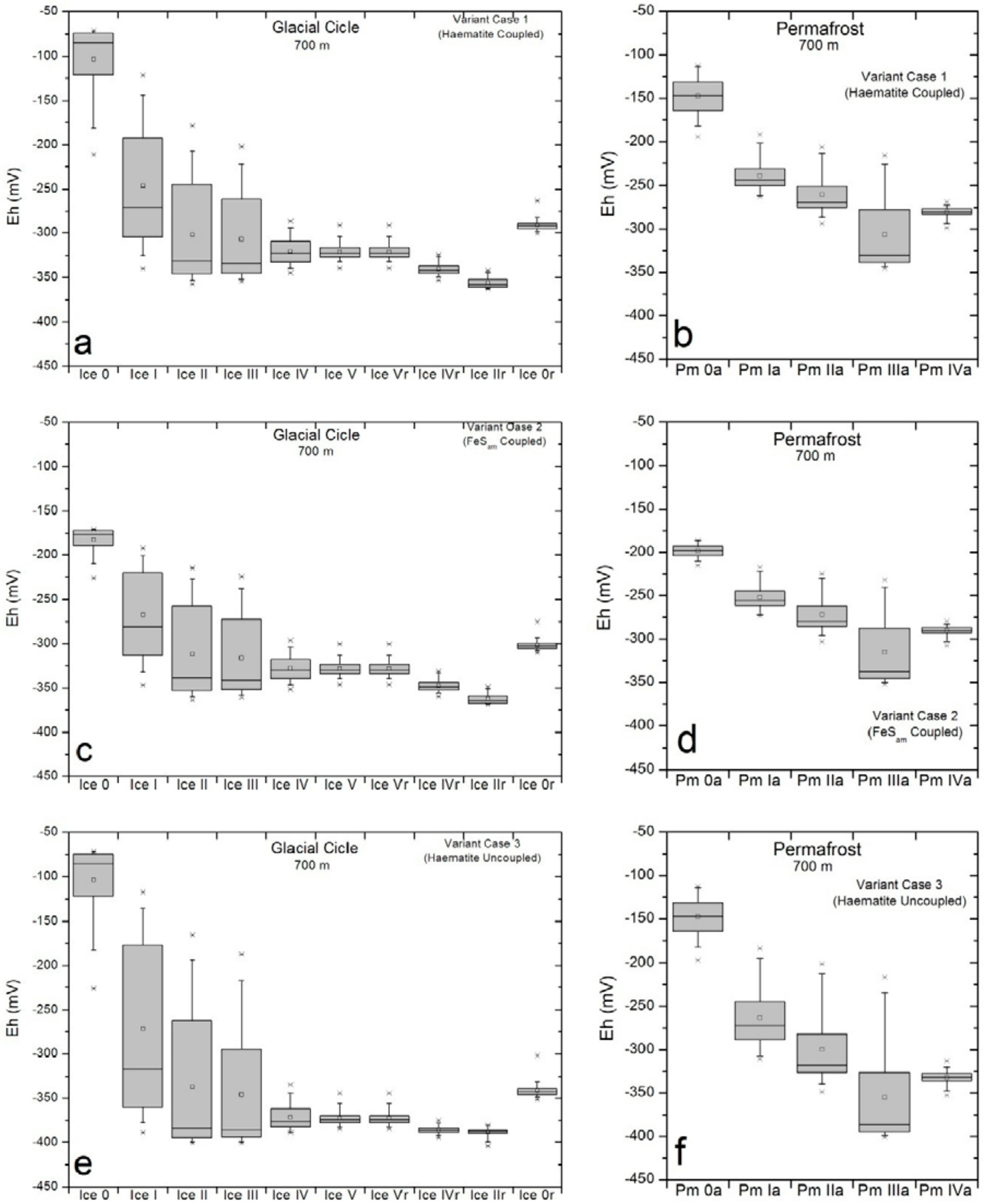

Figure 3-7. *Box-and-whisker plot showing the statistical distribution of Eh (mV) obtained for the different geochemical variant cases (Case 1, a and b, Case 2, c and d, and Case 3, e and f) when considering an ice-sheet advancing over unfrozen ground (a, c) and when considering an ice-sheet advancing over frozen ground (permafrost) (b, d) for the groundwater located within the SE-SFL repository volume at Laxemar at 700 m depth. See the caption of Figure 3-1 for the statistical meaning of the different symbols.*

4 Final remarks

The hydrochemical evolution of the groundwater during periods of periglacial and glacial climate conditions in the rock volume chosen for the safety evaluation SE-SFL (at two depths, 500 and 700 m, in the Laxemar site) has been modelled by coupling fluid flow and solute transport results (Vidstrand et al. 2010), with a geochemical model including mineral reactions. The methodology used was developed for the SR-Can and SR-Site assessments (SKB 2006, 2011). The coupling of the two models allows a description of the geochemical heterogeneity, which otherwise would be hard to attain.

The methodology used involves using the groundwater salinity calculated by a hydrogeological model to determine the mass fractions of three reference waters thought to be present in the system (considered as mixing proportions of end members in the geochemical calculations). The mass fractions of the reference waters are then used to create an input file for the geochemical calculations. Different geochemical variant cases have been defined for calculating the relevant geochemical parameters over the different evolution stages in order to assess their variability under specific hydrogeochemical conditions.

This methodology has a series of uncertainties that are thoroughly described in Gimeno et al. (2010). However, despite the usual constraints associated with predictive numerical models, the main objective of the present work has been achieved. The main results obtained for the geochemical parameters of interest through the different stages of a glacial cycle (with or without permafrost development) are summarised next. The statistical results are compiled in tables in Appendix 2.

During the glacial cycle, salinities are basically controlled by the infiltration of glacial melt waters, the transport of saline waters from the deepest areas by upconing, and the existence (or absence) of a frozen ground (permafrost). The salinity distribution simulated for the Ice 0a stage of the glacial period is assumed to be quite similar to the one obtained for the last year simulated in the temperate period. The general trend is a decrease in the salinity in the entire modelled domain due to the infiltration of glacial melt waters when the glacier advances over an unfrozen soil and even when it retreats. At the end of the glacial cycle the repository volume seems to reach salinity values similar to the ones existing there at the beginning of the glacial cycle.

In general, these conditions affect the geochemistry of the groundwater at the repository volume at 500 m depth quicker than at 700 m. That difference creates a broader range of variation in the values of all the geochemical parameters at 700 m (not only salinity and major chemical components concentrations, but also the pH and the Eh values) and mainly during the first stages of the ice advance (0a to IIIa). Groundwater features stabilise quicker at 500 m depth, usually during stage Ice IIa, whilst the groundwater is still changing at 700 m depth. Then there is a quite stable situation from stage IVa until stage IIr when the retreating ice front becomes close and the evolution continues in the same direction as it had been at the beginning of the ice advance. The final stage analysed here (Ice 0r) shows the return towards similar values as the ones before the onset of the glacial conditions.

With respect to the results obtained when considering permafrost conditions, in general the temporal changes in groundwater chemistry are more moderate (the presence of the frozen ground seems to buffer temporarily the effect of the melt waters infiltration) although there are usually more variation in the results at 700 m and during the stage Pm IVa, probably because is when the dilution effects reach that depth.

These general trends have been observed in all the parameters described in this report: pH, Eh, carbon content and CO_2 partial pressure. They are also observed in the values summarised in the tables in Appendix 2.

With respect to the results obtained with the different geochemical variant cases, they are virtually identical for the non-redox parameters, that is, their values and evolution are independent of the redox controlling processes. However, the Eh results are quite different depending on the redox mineral (haematite or FeS(am)) and on the assumption of redox equilibrium or disequilibrium for the sulfur system. In any case, for all the glacial stages with or without permafrost, the redox potential of the groundwater within the SFL repository domain is expected to be clearly reducing.

Finally some comments can be made when comparing the results obtained for the location chosen for the SE-SFL at 500 m with those obtained for the repository volume evaluated for the spent nuclear fuel repository in SR-Site located at the same depth (Gimeno et al. 2010). The SE-SFL volume is a part of the volume considered in SR-Site and therefore the results obtained in the present study are within the range of results for the SR-Site volume. For some of the ice-front locations evaluated here, the hydrogeological conditions in the SE-SFL volume differ substantially from those at the centre of the SR-Site volume and therefore the results of the geochemical calculations also differ substantially.

One of the main differences occurs in the very first simulation stage of the ice movement (Ice Ia) which, in the case of the SR-Site, always shows the effect of the upconing. This effect is not seen in the first simulated ice margin stage for the SE-SFL volume because the SE-SFL is already under the ice and at some distance to the ice front, as illustrated in Figure 3-1e. However, the upconing effect would have been seen if different locations of the ice front margin had been simulated. The values obtained for all the geochemical parameters starting with the first simulated ice margin stage show a continuous evolution defined by a progressive decrease/increase (depending on the parameter), then a stabilisation of the values and finally another increase/decrease (opposite to the trend at the beginning) after the ice retreat, see Figures 3-1 to 3-7. A similar trend was also shown in the results from SR-Site after the effect of the upconing, but with slightly more extreme values than those found for SE-SFL (higher maximum and lower minimum values), giving a larger range of variation in almost all of the parameters, which might be related to the relative locations of the ice front, the larger repository volume, and the larger number of grid points treated in the SR-site simulations. It is to be expected that substantially larger changes in the geochemical parameters and upconing effects similar to those observed in SR-Site would occur in the SE-SFL rock volume when the ice margin is located exactly on top, although it has not been possible to analyse such a situation in the present study.

Differences between the results for the SE-SFL volume and the SR-Site volume also exist for the case with frozen ground above the repository prior to the ice-sheet advance: 1) the geochemical parameters during the first movement of the ice show a larger change (increase or decrease, depending on the parameter) at the SE-SFL than at the SR-Site; 2) the range of variation for most of the parameters is (as for the case without permafrost) broader for the SR-Site; and 3) specific for the frozen ground case is that the monotonic trend in the geochemical parameters is reversed in the fourth stage of the ice-sheet evolution (Pm IVa), while this reversal does not occur in the case of the SR-Site. Nevertheless, irrespective of these differences, the SE-SFL values are always inside the ranges found for the SR-Site.

5 References

SKB's (Svensk Kärnbränslehantering AB) publications can be found at www.skb.com/publications. SKBdoc documents will be submitted upon request to document@skb.se.

Auqué L F, Gimeno M J, Gómez J B, Puigdomenech I, Smellie J, Tullborg E-L, 2006. Groundwater chemistry around a repository for spent nuclear fuel over a glacial cycle. Evaluation for SR-Can. SKB TR-06-31, Svensk Kärnbränslehantering AB.

Elfwing M, Evins L Z, Gontier M, Grahm P, Mårtensson P, Tunbrant S, 2013. SFL concept study. Main report. SKB TR-13-14**,** Svensk Kärnbränslehantering AB.

Gimeno M J, Auqué L F, Gómez J, Acero P, 2008. Water–rock interaction modelling and uncertainties of mixing modelling. SDM-Site Forsmark. SKB R-08-86, Svensk Kärnbränslehantering AB.

Gimeno M J, Auqué L F, Gómez J, Acero P, 2009. Water–rock interaction modelling and uncertainties of mixing modelling. SDM-Site Laxemar. SKB R-08-110, Svensk Kärnbränslehantering AB.

Gimeno M J, Auqué L F, Gómez J, Salas J, Molinero J, 2010. Hydrogeochemical evolution of the Laxemar Site. SKB R-10-60, Svensk Kärnbränslehantering AB.

Gimeno M J, Auqué L F, Acero P, Gómez J B, 2014. Hydrogeochemical characterisation and modelling of groundwaters in a potential geological repository for spent nuclear fuel in crystalline rocks (Laxemar, Sweden). Applied Geochemistry 45, 50–71.

Gómez J B, Gimeno M J, Auqué L F, Acero P, 2014. Characterisation and modelling of mixing processes in groundwaters of a potential geological repository for nuclear wastes in crystalline rocks of Sweden. Science of the Total Environment 468–469, 791–803.

Joyce S, Simpson T, Hartley L, Applegate D, Hoek J, Jackson P, Roberts D, Swan D, Gylling B, Marsic N, Rhén I, 2010. Groundwater flow modelling of periods with temperate climate conditions – Laxemar. SKB R-09-24, Svensk Kärnbränslehantering AB.

Joyce S, Appleyard P, Hartley L, Tsitsopoulos V, Woollard H, Marsic N, Sidborn M, Crawford J, 2019. SFL Groundwater flow modelling of temperate conditions. SKB R-19-02, Svensk Kärnbränslehantering AB.

Laaksoharju M, Smelie J, Tullborg E-L, Wallin B, Drake H, Gascoyne M, Gimeno M, Gurban, I, Hallbeck L, Molinero J, Nilsson A-C, Waber N, 2009. Bedrock hydrogeochemistry, Laxemar. Site descriptive modelling. SDM-Site Laxemar. SKB R-08-93, Svensk Kärnbränslehantering AB.

OriginLab Corporation, 2007. Origin. Scientific graphing and analysis software. OriginPro 8 SR0 v8.0724 (B724)**.** Commercial. Northampton, MA: OriginLab Corporation.

Parkhurst D L, Appelo C A J, 2013. Description of input and examples for PHREEQC version 3 – A computer program for speciation, batch-reaction, one-dimensional transport, and inverse geochemical calculations. Techniques and Methods 6–A43, U.S. Geological Survey, Denver, Colorado.

Salas J, Gimeno M J, Molinero J, Auqué L F, Gómez J, Juárez I, 2010. SR-Site – hydrogeochemical evolution of the Forsmark site. SKB TR-10-58, Svensk Kärnbränslehantering AB.

Selroos J-O, Follin S, 2010. SR-Site groundwater flow modelling methodology, setup and results. SKB R-09-22, Svensk Kärnbränslehantering AB.

SKB, 2006. Climate and climate-related issues for the safety assessment SR-Can. SKB TR-06-23, Svensk Kärnbränslehantering AB.

SKB, 2011. Long-term safety for the final repository for spent nuclear fuel at Forsmark. Main report of the SR-Site project. SKB TR-11-01, Svensk Kärnbränslehantering AB.

SKB, 2013. Thermodynamic database_ TDB_SKB-2009_Amphos21. SKBdoc 1261302 ver 3.0, Svensk Kärnbränslehantering AB.

Vidstrand P, Follin S, Zugec N, 2010. Groundwater flow modelling of periods with periglacial and glacial conditions – Laxemar. SKB R-09-25, Svensk Kärnbränslehantering AB.

Appendix 1

Calculation procedure

Based on the software developed by the University of Zaragoza for the SR-Site calculations, some updates were performed to be compatible with the new versions of the geochemical program and the thermodynamic database. The PHREEQC version used for these calculations is PHREEQC 3.3, batch version 3.3.5.10806. The thermodynamic database (SKB 2013) is the one used by Joyce et al. (2019) for the modelling of temperate conditions at the location chosen for the safety evaluation SE-SFL (SKB-2009_vers-3_SFL-modified_150528.dat). This database is essentially the same as the one used by Salas et al. (2010) and Gimeno et al. (2010) for the SR-Site calculations with some corrections and updates (see Chapter 2). However, these updates have not changed the basic principles of the former versions used for SR-Site that are described in Appendix 1 of Gimeno et al. (2010).

The main difference with the procedure followed in SR-Site is that, in order to automatise the calculations, most of the steps are now included in two Windows scripts that are presented in this appendix: slice_creator.cmd and make_SFL.cmd. The first one automatises the slice extraction procedure from the hydrological data and the conversion of the salinity data into mixing proportions. The second script creates the input files for PHREEQC, runs PHREEQC, and creates the output files with the key geochemical parameters to be used in SE-SFL. All the programs and necessary files are described next.

A1.1 Root folder, subfolders, programs and data files

All paths in both scripts are relative paths with respect to a root folder whose name can be chosen arbitrarily. This root folder (e.g. in the example shown here \SFL\) *must* contain the following sub-folders, programs and data files:

1. Sub-folders:
    - \GnuWin32\: this subfolder contains the zip.exe program to compress PHREEQC input and output files.
    - \Hydrofiles\: this subfolder contains the data files provided by the hydrogelogists, one for each simulation stage. The input data files have names matching the template SFL_xa_bb.txt (where a, b, and x have the meaning explained below).
    - \SliceCreator\: subfolder containing the java program SelectData.jar, called by script slice_creator.cmd to perform the extraction of slices from the hydrogeology data files. Program Select_Data.jar needs java 6.0 or above to run.
    - \Slices\: this subfolder will be filled in by the script slice_creator.cmd that creates the different cuts extracted from the original data files provided by the hydrogeologists. Before running this script, the subfolder should contain two auxiliary data files to be used by the script slice_creator.cmd: SFL.bln (with the coordinates of the repository volume), and SFL_v135.bln (with the orientation of the vertical cut in the direction N135E). Both files are used by java program Select_Data.jar (as explained below).
2. Programs:
    a. the two script files: slice_creator.cmd and make_SFL.cmd,
    b. the program Salinity2Mixprop.exe: to transform the salinity values included in the hydro-files into mixing proportions in the cut files (this program needs salflibc.dll in the root folder to run),
    c. the program create_pqi.exe (to create the .pqi input data for PHREEQC; this program needs salflibc.dll in the root folder to run), and
    d. the program phreeqc.exe batch version (it creates *.pqo and *.prn selected output files).
3. Auxiliary data files:
    a. Equilibrium phases data file: it contains the phases with which equilibrium is attained in the simulations (used by create_pqi.exe). Accepted names: SFL_Eq_FeOx.dat, SFL_aFeS.dat (for the equilibrium with haematite or the ferrous iron monosulfide, respectively; see Section A1.5.1).
    b. Selected output data file: it contains the instructions that PHREEQC needs to create a selected output with the needed geochemical information (used by create_pqi.exe). Accepted names: SFL_sel_c.dat, SFL_sel_u.dat (for the different type of results obtained when using the coupled or the uncoupled thermodynamic database, respectively; see Section A1.5.2).

c. End-members data file: it contains the chemical composition of the end-member waters (necessary for create_pqi.exe). Accepted names: SFL_em_c.dat, and SFL_em_u.dat (for the end members equilibrated using the coupled or the uncoupled database, respectively; see Section A1.5.3).

d. Thermodynamic data base (used by phreeqc.exe). Accepted names: TDB_SKB-2009_vers-3_SFL-modified_150528.dat, and TDB_SKB-2009_vers-3_SFL-modified_no_CH4_N2_S-redox_20160229.dat (these files are too long to be included in this Appendix).

All folders and auxiliary data files have strict naming conventions that are constructed by the scripts piece by piece in such a way that no user intervention is necessary. The following sections briefly explained the basic functioning of each script.

A1.2 Script for the slices extraction: slice_creator.cmd

This script automatically extracts and organises in folders the appropriate "cuts" from the original data files provided by the hydrogeologists, and then transforms the salinity data into mixing proportions. All folders and cut files have strict naming conventions that this script constructs piece by piece (no user-input is necessary).

As indicated above, there *must* be a folder named Hydrofiles, hanging directly from the root folder, where all the input data files provided by the hydrogeologists should be stored. If script slice_creator.cmd does not find the subfolder and/or the data files, an error message will appear on the screen.

Additionally, the folder named \Slices\ must exist before the script is run and contain the two auxiliary files SFL.bln and SFL_v135.bln.

The script creates 5 subfolders inside folder \Slices\ with the following specific names where the different "cuts" are stored:

- \h500_all\: horizontal plane at 500 m depth,
- \h500_rep\: repository volume at 500 m depth,
- \h700_all\: horizontal plane at 700 m depth,
- \h700_rep\: repository volume at 700 m depth, and
- \v135_all\: vertical plane with the direction N135E.

Once the cuts are extracted, they are processed by the program Salinity2Mixprop.exe (use by this script), that converts the salinity data into mixing proportions.

All the names of the created cut files follow the template SFL_xa_bb_cyyy_ddd where letters a through d stand for specific alphabetic characters and letters x and y stand for specific numeric characters:

- x: simulation time stage (accepted values: 0, 1, 2, 3, 4, 5),
- a: advancing or retreating ice sub-stage (accepted values: a, r) (a is for advancing ice; r is for retreating ice),
- bb: simulation case (accepted values: gl, pm) (gl – glacial – is the base case; pm – permafrost – is the variant case),
- c: orientation of the hydro-file section (accepted values: h, v) (h is for horizontal sections and v for vertical sections),
- yyy: depth (for horizontal sections) or orientation (for vertical sections) of the hydro-file cut (accepted values: 500, 700, 135, 045) (500 and 700 are for the horizontal cuts; 135, meaning N135E, is for the vertical cut), and
- ddd: volume of the extracted sections (accepted values: all, rep) (all is for the complete horizontal plane at a specific depth and rep is for the repository volume).

These cut files have two different endings and are stored in different folders (inside each cut subfolder):

- .txt for cuts with salinity data. These files are stored in folders with the following naming convention: bb_cyyy_ddd (where letters b, c, d, and y have the same meaning as above).

- .txt.res for cut files processed by program Salinity2Mixprop.exe (used by this script), that converts salinity data into mixing proportions. These files are stored in folders with the following naming conventions: MixProp_bb_cyyy_ddd (where letters b, c, d, x, and y have the same meaning as above).

After running batch file slice_creator.cmd, the tree of folders and the files thus created are used by the script make_SFL.cmd to perform the needed PHREEQC simulations. This script is described below.

A1.3 Script for the PHREEQC calculations: make_SFL.cmd

Before this script is run the user should have run the script slice_creator.cmd to extract the specific “cuts”. Then, the script make_SFL.cmd (1) automatically creates *.pqi input data files for SFL PHREEQC simulations using the different “cuts” of the files provided by the hydrogeologists; (2) runs PHREEQC simulations with these input files, and (3) produces tailored output files (selected output) with all the relevant physico-chemical information in a *.prn text file.

The PHREEQC *.pqi input files and *.pqo and *.prn output files have names with the following parts: SFL_xa_bb_cyyy_ddd_e_ffff where letters a through f stand for specific alphabetic characters and letters x and y stand for specific numeric characters:

- x: simulation time stage (accepted values: 0, 1, 2, 3, 4, 5),
- a: advancing or retreating ice sub-stage (accepted values: a, r) (a is for advancing ice; r is for retreating ice),
- bb: simulation case (accepted values: gl, pm) (gl – glacial – is the base case; pm – permafrost – is the variant case),
- c: orientation of the hydro-file section (accepted values: h, v) (h is for horizontal sections and v for vertical sections),
- yyy: depth (for horizontal sections) or orientation (for vertical sections) of the hydro-file cut (accepted values: 500, 700, 135, 045) (500 and 700 are for the horizontal cuts; 135, meaning N135E, and 045 are for the vertical cuts), and
- ddd: volume of the extracted sections (accepted values: all, rep) (all is for the complete horizontal plane at a specific depth and rep is for the repository volume);
- e: type of thermodynamic data base (accepted values: u, c) (u is for an un-coupled database; c is for a coupled database);
- ffff: iron phase to attain equilibrium with (accepted values: FeOx, aFeS) (FeOx is a ferric oxide; aFeS is an amorphous ferrous monosulfide).

The script stores all output files in different subfolders hanging from the root folder. Each subfolder contains all the output files of a specific simulation stage, ten in total: \SFL_0a\, \SFL_1a\, \SFL_2a\, \SFL_3a\, \SFL_4a\, \SFL_5a\, \SFL_5r\, \SFL_4r\, \SFL_2r\, and \SFL_0r\. The names have been written in temporal order (0a being the first stage and 0r the last stage).

Important note: the list of simulations to be performed by script make_SFL.cmd is written in a SET sentence in line number 60:

SET “list_of_simulations= SFL_0a_gl_h500_all_c_FeOx, SFL_0a_gl_h500_all_c_aFe, ...”.

As the total list of simulations is rather long, we have decided to separate them into different scripts, one for each temporal stage (0a, 1a, 2a, etc). Thus, the following script variants have been created, each one performing the simulations for a specific stage:

make_SFL_0a.cmd, make_SFL_1a.cmd, make_SFL_2a.cmd, make_SFL_3a.cmd, make_SFL_4a.cmd, make_SFL_5a.cmd, make_SFL_5r.cmd, make_SFL_4r.cmd, make_SFL_2r.cmd, make_SFL_0r.cmd.

Figure A1-1 shows the complete list of folders, programs and auxiliary files that the root folder would contain after running both script files.

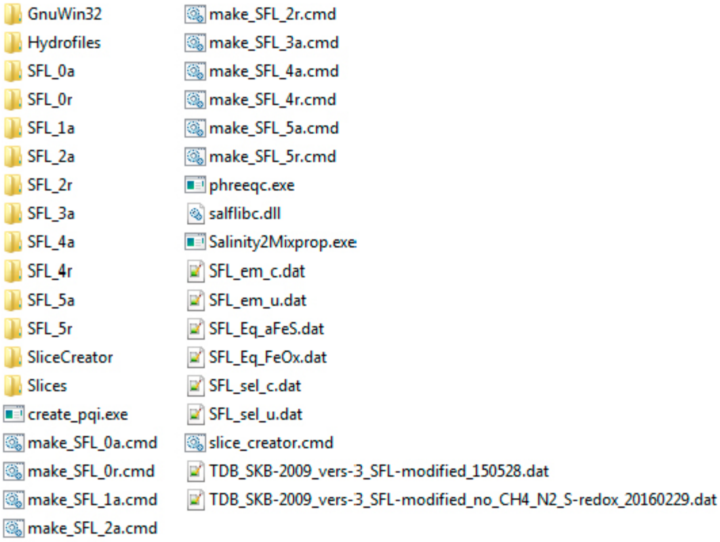

GnuWin32
Hydrofiles
SFL_0a
SFL_0r
SFL_1a
SFL_2a
SFL_2r
SFL_3a
SFL_4a
SFL_4r
SFL_5a
SFL_5r
SliceCreator
Slices
create_pqi.exe
make_SFL_0a.cmd
make_SFL_0r.cmd
make_SFL_1a.cmd
make_SFL_2a.cmd
make_SFL_2r.cmd
make_SFL_3a.cmd
make_SFL_4a.cmd
make_SFL_4r.cmd
make_SFL_5a.cmd
make_SFL_5r.cmd
phreeqc.exe
salflibc.dll
Salinity2Mixprop.exe
SFL_em_c.dat
SFL_em_u.dat
SFL_Eq_aFeS.dat
SFL_Eq_FeOx.dat
SFL_sel_c.dat
SFL_sel_u.dat
slice_creator.cmd
TDB_SKB-2009_vers-3_SFL-modified_150528.dat
TDB_SKB-2009_vers-3_SFL-modified_no_CH4_N2_S-redox_20160229.dat

Figure A1-1. *List of folders, programs and auxiliary files that the root folder would contain after running both script files.*

A1.4 Postprocessing the results

In the case of the repository domain calculations (data points within the SE-SFL repository volumes at 500 and 700 m depth), the selected results have been treated with specific statistical analysis. In these cases, the post-processing has been performed by “Box-and-whisker plots”, using OriginPro 8 SR0 v8.0724 (B724; OriginLab Corporation 2007), showing the statistical distribution of the chosen parameters and the main statistical values are shown in Tables in Appendix 2.

A1.5 Auxiliary files

As indicated above, to create the PHREEQC input and output files (apart from the hydro file with the mixing proportions calculated at each point) several auxiliary files are needed:

1. the file containing the names of the end members to be mixed and the mineral phases to be equilibrated (Equilibrium phases data file),
2. the file with the complete chemical composition of the end members (End members data file),
3. the file with the thermodynamic database to be used for the calculations, and
4. to obtain the selected output, an additional file has been created to be written inside the PHREEQC input file, indicating the parameters to be extracted from the output files.

The user must keep these files updated for each specific problem to be solved (different end members, different equilibrium minerals, different elements or minerals to be obtained in the selected output, different thermodynamic databases, etc.).

All the auxiliary files, except the thermodynamic databases (which are too long) are written below.

A1.5.1 Equilibrium phases data files

SFL_Eq_aFeS.dat

```
3   !Number of end members, followed by their names
"Brine" "Meteoric" "Glacial"
3   !Number of phases for equilibrium calculations
"Calcite" 0 10
"Quartz" 0 10
"FeS(ppt)" 0 10
0   !número de intercambiadores (para intercambio catiónico)
```

SFL_Eq_FeOx.dat

```
3   !Number of end members, followed by their names
"Brine" "Meteoric" "Glacial"
3   !Number of phases for equilibrium calculations
"Calcite" 0 10
"Quartz" 0 10
"Fe(OH)3(hematite_grenthe)" 0 10
0   !número de intercambiadores (para intercambio catiónico)
```

A1.5.2 Selected Output data files

The information selected to be extracted with the following selected output options include:

- X, Y, Z coordinates[1]
- Mixing proportions of the end-member waters for each point: Deep Saline, Glacial and Altered Meteoric.
- Mass transfers for the equilibrated minerals.
- TDS
- Molality of the elements included in the selected output's format file: result of mixing and reaction.
- pH, pe, ionic strength, total alkalinity, charge balance.
- Activity and molality of the selected species.
- Saturation indexes of the waters with respect to the selected mineral phases.

File SFL_sel_c.dat

```
CALCULATE_VALUES
TDS_mgL
-start
 10 main_c = TOT("K")*39.1+TOT("Sr")*87.6+TOT("Na")*22.99+TOT("Ca")*40.08+TOT(
"Mg")*24.31
 15 other_c = TOT("Mn")*54.94+TOT("Si")*60.08+TOT("Fe")*55.85+TOT("Li")*6.941
 20 main_a = TOT("I")*126.9+TOT("Cl")*35.45+TOT("Br")*79.9+TOT("F")*19+TOT
("S(6)")*96.06
 25 other_a = TOT("C(4)")*60.01+TOT("N(-3)")*17.03+TOT("N(3)")*46.01+TOT
("N(5)")*62+ +TOT("P")*95
 30 x = MOL("H+")*1.0079+MOL("OH-")*17.01
 35 tds = other_c + other_a + x + main_c + main_a
100 SAVE 1000*tds
-end
Eh(Fe(2)/Fe(3))_mV
-start
 50 slope = LOG(10)*8.31451*TK/96485.309
 55 e0_fe = -slope*(LK_SPECIES("Fe+3"))
 60 eh_fe = -0.99999
 65 IF LA("Fe+2") > -99. THEN eh_fe = e0_fe - slope*(LA("Fe+2")-LA("Fe+3"))
 70 SAVE 1000*eh_fe
-end
pe(Fe(2)/Fe(3))
-start
 50 slope = LOG(10)*8.31451*TK/96485.309
 55 e0_fe = -slope*(LK_SPECIES("Fe+3"))
 60 eh_fe = -0.99999
 65 IF LA("Fe+2") > -99. THEN eh_fe = e0_fe - slope*(LA("Fe+2")-LA("Fe+3"))
 70 SAVE (eh_fe/slope)
-end
```

---

[1] The distance along the line calculated for the vertical plane is not stored here as it is not included in the PHREEQC output; therefore if the user wants to plot spatial distributions, this value must be calculated again using the following equation: $\text{Distance} = \sqrt{X^2 + Y^2}$.

```
EhFeOxOH_mV
-start
 50 slope = LOG(10)*8.31451*TK/96485.309
 80 e0_fe = -slope*(LK_SPECIES("Fe+3")-LK_PHASE("Fe(OH)3(hematite_grenthe)"))
 85 eh_fe = -999.999
 90 IF LA("Fe+2") > -99. THEN eh_fe = e0_fe - slope*(-3*LA("H+")+LA("Fe+2"))
100 SAVE 1000*eh_fe
-end
Eh_mV
-start
10 SAVE (-LA("e-")*8.31451*TK*LOG(10)/96485.309)*1000
-end
Eh(HS/SO4)_mV
-start
 50 slope = LOG(10)*8.31451*TK/96485.309
 55 e0_S = (1/8)*slope*(LK_SPECIES("HS-"))
 60 eh_S = -0.99999
 65 IF LA("HS-") > -99. THEN eh_S = e0_S +
(slope/8)*(-LA("HS-")+LA("SO4-2")+9*LA("H+"))
 70 SAVE 1000*eh_S
-end

SELECTED_OUTPUT 1
   -file                 SELECTED_OUTPUT.prn
   -reset                false
   -pH                   true
   -pe                   true
   -alkalinity           true
   -ionic_strength       true
   -totals               Al  Ca  Mg  Na  K  Cl  C
                         S(6)  S(-2)  Fe(2)  Fe(3)  Mn  Si  Sr
                         F  Li  Br
   -activities           Si(OH)4  Ca+2  Mg+2  Na+
                         K+  Al+3  H+  Fe+2
                         Fe+3  HS-  H2S  HCO3-
   -equilibrium_phases   Calcite  Quartz  Fe(OH)3(hematite_grenthe)  FeS(ppt)
   -saturation_indices   Calcite  Rhodochrosite  Siderite  Quartz
                         Fe(OH)3(hematite_grenthe)  Fe(OH)3(mic)  Fe(OH)3(am)
FeS(ppt)
                         Fluorite  Strontianite  Celestite  Albite
                         K-feldspar  Kaolinite_Grimaud  CO2(g)  Gypsum
   -calculate_values     Eh(Fe(2)/Fe(3))_mV  pe(Fe(2)/Fe(3))  EhFeOxOH_mV  Eh_mV
                         Eh(HS/SO4)_mV  TDS_mgL
   -active               true
   -user_punch           true
```

File SFL_sel_u.dat

```
CALCULATE_VALUES
TDS_mgL
-start
 10 main_c = TOT("K")*39.1+TOT("Sr")*87.6+TOT("Na")*22.99+TOT("Ca")*40.08+TOT(
"Mg")*24.31
 15 other_c = TOT("Mn")*54.94+TOT("Si")*60.08+TOT("Fe")*55.85+TOT("Li")*6.941
 20 main_a = TOT("I")*126.9+TOT("Cl")*35.45+TOT("Br")*79.9+TOT("F")*19+TOT
("S(6)")*96.06
 25 other_a = TOT("C(4)")*60.01+TOT("N(-3)")*17.03+TOT("N(3)")*46.01+TOT
("N(5)")*62+ +TOT("P")*95
 30 x = MOL("H+")*1.0079+MOL("OH-")*17.01
 35 tds = other_c + other_a + x + main_c + main_a
100 SAVE 1000*tds
-end
```

```
Eh(Fe(2)/Fe(3))_mV
-start
 50 slope = LOG(10)*8.31451*TK/96485.309
 55 e0_fe = -slope*(LK_SPECIES("Fe+3"))
 60 eh_fe = -0.99999
 65 IF LA("Fe+2") > -99. THEN eh_fe = e0_fe - slope*(LA("Fe+2")-LA("Fe+3"))
 70 SAVE 1000*eh_fe
-end
pe(Fe(2)/Fe(3))
-start
 50 slope = LOG(10)*8.31451*TK/96485.309
 55 e0_fe = -slope*(LK_SPECIES("Fe+3"))
 60 eh_fe = -0.99999
 65 IF LA("Fe+2") > -99. THEN eh_fe = e0_fe - slope*(LA("Fe+2")-LA("Fe+3"))
 70 SAVE (eh_fe/slope)
-end
EhFeOxOH_mV
-start
 50 slope = LOG(10)*8.31451*TK/96485.309
 80 e0_fe = -slope*(LK_SPECIES("Fe+3")-LK_PHASE("Fe(OH)3(hematite_grenthe)"))
 85 eh_fe = -999.999
 90 IF LA("Fe+2") > -99. THEN eh_fe = e0_fe - slope*(-3*LA("H+")+LA("Fe+2"))
100 SAVE 1000*eh_fe
-end
Eh_mV
-start
10 SAVE (-LA("e-")*8.31451*TK*LOG(10)/96485.309)*1000
-end
Eh(HS_/SO4)_mV
-start
 50 slope = LOG(10)*8.31451*TK/96485.309
 55 e0_S = (1/8)*slope*(LK_SPECIES("HS_-"))
 60 eh_S = -0.99999
 65 IF LA("HS_-") > -99. THEN eh_S = e0_S +
(slope/8)*(-LA("HS_-")+LA("SO4-2")+9*LA("H+"))
 70 SAVE 1000*eh_S
-end

SELECTED_OUTPUT 1
   -file                 SELECTED_OUTPUT.prn
   -reset                false
   -pH                   true
   -pe                   true
   -alkalinity           true
   -ionic_strength       true
   -totals               Al  Ca  Mg  Na  K  Cl  C
                         S(6)  S_(-2)  Fe(2)  Fe(3)  Mn  Si  Sr
                         F  Li  Br
   -activities           Si(OH)4  Ca+2  Mg+2  Na+
                         K+  Al+3  H+  Fe+2
                         Fe+3  HS_-  H2S_  HCO3-
   -equilibrium_phases   Calcite  Quartz  Fe(OH)3(hematite_grenthe)
                         FeS_(ppt)
   -saturation_indices   Calcite  Rhodochrosite  Siderite  Quartz
                         Fe(OH)3(hematite_grenthe)  Fe(OH)3(mic)
                         Fe(OH)3(am)  FeS_(ppt)
                         Fluorite  Strontianite  Celestite  Albite
                         K-feldspar  Kaolinite_Grimaud  CO2(g)
                         Gypsum
   -calculate_values     Eh(Fe(2)/Fe(3))_mV  pe(Fe(2)/Fe(3))
                         EhFeOxOH_mV  Eh_mV
                         Eh(HS_/SO4)_mV  TDS_mgL
   -active               true
   -user_punch           true
```

A1.5.3 End members data files

`SFL_em_c.dat`

```
SOLUTION 1 SFL Deep Saline
    temp      15
    pH        8
    pe        -4.448
    redox     pe
    units     mol/kgw
    density   1
    Al        7.382e-09
    Br        0.004156
    C         3.682e-05
    Ca        0.494
    Cl        1.354
    F         8.644e-05
    Fe        2.665e-07
    K         0.0008217
    Li        0.0006861
    Mg        8.952e-05
    Mn        2.615e-06
    Na        0.3801
    S         0.009679
    Si        8.822e-05
    Sr        0.003947
    -water    1 # kg

SOLUTION 2 SFL AlteredMeteoric
    temp      15
    pH        7.842
    pe        -1.046
    redox     pe
    units     mol/kgw
    density   1
    Al        2.031e-07
    C         0.004259
    Ca        0.0001785
    Cl        0.0004322
    F         0.0002027
    Fe        1.792e-06
    K         7.6e-05
    Li        1.586e-06
    Mg        0.0001482
    Mn        1.056e-06
    Na        0.004787
    S         0.0003728
    Si        0.0001354
    -water    1 # kg

SOLUTION 3 SFL Glacial (calcite-1)
    temp      15
    pH        9.30
    pe        -5.260
    redox     pe
    units     mol/kgw
    density   1
    Al        5.207e-06
    C         8.517e-05
    Ca        7.182e-05
    Cl        2.246e-05
    Fe        8.002e-07
    K         1.023e-05
    Mg        4.114e-06
    Na        7.395e-06
    S         5.305e-06
    Si        0.0001665
    -water    1 # kg
END
```

SFL_em_u.dat

```
SOLUTION 1 SFL DeepSaline
    temp      15
    pH        8
    pe        -5.204
    redox     pe
    units     mol/kgw
    density   1
    Al        7.382e-09
    Br        0.004156
    C         3.682e-05
    Ca        0.494
    Cl        1.354
    F         8.644e-05
    Fe        1.431e-06
    K         0.0008216
    Li        0.0006861
    Mg        8.952e-05
    Mn        2.615e-06
    Na        0.38
    S         0.009679
    S_        1.026e-15
    Si        8.822e-05
    Sr        0.003947
    -water    1 # kg

SOLUTION 2 SFL AlteredMeteoric
    temp      15
    pH        7.842
    pe        -1.046
    redox     pe
    units     mol/kgw
    density   1
    Al        2.031e-07
    C         0.004259
    Ca        0.0001785
    Cl        0.0004322
    F         0.0002027
    Fe        1.792e-06
    K         7.6e-05
    Li        1.586e-06
    Mg        0.0001482
    Mn        1.056e-06
    Na        0.004787
    S         0.0003728
    S_        1e-15
    Si        0.0001354
    -water    1 # kg

SOLUTION 3 SFL Glacial
    temp      15
    pH        9.29
    pe        -2.614
    redox     pe
    units     mol/kgw
    density   1
    Al        5.09e-06
    C         8.616e-05
    Ca        7.232e-05
    Cl        2.028e-05
    Fe        3.247e-09
    K         1.023e-05
    Mg        4.114e-06
    Na        7.395e-06
    S         6.246e-06
    S_        1e-07
    Si        0.0001658
    -water    1 # kg
END
```

Appendix 2

Tables with the statistical results

This appendix lists the statistical results obtained for the main geochemical parameters for all the periods simulated over a complete glacial cycle. The results correspond to the geochemical Base Case simulations over the grid points inside the repository volume at 500 m (Tables A2-1 and A2-2) and at 700 m (Tables A2-3 and A2-4).

Table A2-1. Statistical results for the main geochemical parameters obtained with the geochemical Base Case over the glacial period when considering an ice-sheet advancing over unfrozen ground in the repository volume at 500 m depth. Chemical components in mol/kg, TDS in mg/L, pH in standard units and Eh in mV.

Repository 500 m (Glacial)
Base Case

Glacial 0 advance	**pH**	**Eh (mV)**	**TDS**	**Ionic Strength**	**Alkalinity**	**C**	**Cl**	**S(6)**	**Ca**	**Mg**	**Na**	**K**	**Si**
Mean	7.50	−221.27	846.73	1.55E−02	3.78E−03	4.07E−03	7.76E−03	4.23E−04	2.68E−03	1.48E−04	6.82E−03	8.00E−05	1.35E−04
Standard Deviation	0.26	25.16	650.70	1.53E−02	3.67E−04	2.01E−04	1.16E−02	7.97E−05	4.08E−03	5.03E−07	3.21E−03	6.38E−06	7.76E−07
Minimum	6.70	−257.37	486.18	7.16E−03	2.46E−03	3.27E−03	1.13E−03	3.77E−04	4.69E−04	1.44E−04	4.98E−03	7.64E−05	1.30E−04
P0.1	6.71	−257.37	486.18	7.16E−03	2.46E−03	3.27E−03	1.13E−03	3.77E−04	4.69E−04	1.44E−04	4.98E−03	7.64E−05	1.30E−04
P5	6.93	−246.74	512.54	7.75E−03	2.93E−03	3.60E−03	1.65E−03	3.81E−04	6.23E−04	1.47E−04	5.13E−03	7.67E−05	1.33E−04
Median	7.57	−227.20	612.11	1.00E−02	3.92E−03	4.14E−03	3.57E−03	3.94E−04	1.22E−03	1.48E−04	5.66E−03	7.77E−05	1.35E−04
P95	7.82	−158.19	2150.00	4.61E−02	4.14E−03	4.25E−03	3.11E−02	5.84E−04	1.08E−02	1.48E−04	1.33E−02	9.29E−05	1.35E−04
P99.9	7.94	−103.49	5727.90	1.31E−01	4.21E−03	4.29E−03	9.37E−02	1.01E−03	3.35E−02	1.48E−04	3.06E−02	1.27E−04	1.36E−04
Maximum	7.94	−101.41	5727.90	1.31E−01	4.21E−03	4.29E−03	9.37E−02	1.01E−03	3.35E−02	1.48E−04	3.06E−02	1.27E−04	1.36E−04
Glacial 1 advance	**pH**	**Eh (mV)**	**TDS**	**Ionic Strength**	**Alkalinity**	**C**	**Cl**	**S(6)**	**Ca**	**Mg**	**Na**	**K**	**Si**
Mean	8.24	−273.26	320.35	5.77E−03	1.69E−03	1.70E−03	2.56E−03	1.65E−04	9.72E−04	6.04E−05	2.54E−03	3.73E−05	1.39E−04
Standard Deviation	0.43	29.90	294.41	6.34E−03	9.45E−04	1.03E−03	4.40E−03	1.07E−04	1.54E−03	3.70E−05	1.96E−03	1.77E−05	4.29E−06
Minimum	6.89	−346.93	62.58	1.11E−03	2.85E−04	2.16E−04	3.89E−04	2.35E−05	2.34E−04	8.43E−06	3.21E−04	1.28E−05	1.33E−04
P0.1	6.90	−339.87	62.58	1.11E−03	2.85E−04	2.16E−04	3.89E−04	2.35E−05	2.34E−04	8.43E−06	3.21E−04	1.28E−05	1.33E−04
P5	7.49	−317.26	107.98	1.92E−03	5.08E−04	4.57E−04	6.10E−04	4.53E−05	3.00E−04	1.72E−05	7.04E−04	1.70E−05	1.35E−04
Median	8.34	−278.67	222.20	3.65E−03	1.43E−03	1.39E−03	1.05E−03	1.31E−04	4.55E−04	4.84E−05	1.84E−03	3.13E−05	1.39E−04
P95	8.87	−220.65	768.18	1.43E−02	3.86E−03	4.11E−03	8.80E−03	3.93E−04	3.12E−03	1.48E−04	5.85E−03	7.76E−05	1.48E−04
P99.9	9.28	−138.23	2458.10	5.34E−02	4.21E−03	4.29E−03	3.66E−02	6.21E−04	1.28E−02	1.48E−04	1.48E−02	9.59E−05	1.66E−04
Maximum	9.29	−136.00	2458.10	5.34E−02	4.21E−03	4.29E−03	3.66E−02	6.21E−04	1.28E−02	1.48E−04	1.48E−02	9.59E−05	1.66E−04
Glacial 2 advance	**pH**	**Eh (mV)**	**TDS**	**Ionic Strength**	**Alkalinity**	**C**	**Cl**	**S(6)**	**Ca**	**Mg**	**Na**	**K**	**Si**
Mean	8.82	−312.04	124.41	2.11E−03	8.33E−04	7.75E−04	7.01E−04	6.84E−05	3.34E−04	2.72E−05	9.45E−04	2.11E−05	1.48E−04
Standard Deviation	0.25	17.43	44.54	7.56E−04	4.06E−04	4.18E−04	4.49E−04	3.58E−05	1.56E−04	1.42E−05	4.64E−04	6.45E−06	7.41E−06
Minimum	8.10	−356.71	59.05	1.06E−03	2.50E−04	1.70E−04	3.86E−04	1.44E−05	2.34E−04	6.27E−06	2.25E−04	1.15E−05	1.37E−04
P0.1	8.10	−355.08	59.05	1.06E−03	2.50E−04	1.70E−04	3.86E−04	1.44E−05	2.34E−04	6.27E−06	2.25E−04	1.15E−05	1.37E−04
P5	8.40	−342.74	72.67	1.30E−03	2.98E−04	2.11E−04	4.14E−04	2.09E−05	2.36E−04	8.02E−06	3.60E−04	1.25E−05	1.40E−04
Median	8.82	−312.11	113.69	1.92E−03	7.73E−04	7.06E−04	6.01E−04	6.23E−05	2.96E−04	2.47E−05	8.54E−04	2.00E−05	1.46E−04
P95	9.25	−282.68	212.67	3.69E−03	1.56E−03	1.52E−03	1.25E−03	1.31E−04	5.22E−04	5.21E−05	1.79E−03	3.24E−05	1.64E−04
P99.9	9.42	−263.79	371.64	6.97E−03	3.24E−03	3.26E−03	4.75E−03	2.84E−04	1.77E−03	1.12E−04	3.74E−03	5.98E−05	1.77E−04
Maximum	9.43	−257.86	371.64	6.97E−03	3.24E−03	3.26E−03	4.75E−03	2.84E−04	1.77E−03	1.12E−04	3.74E−03	5.98E−05	1.77E−04

Table A2-1. Continuation.

Repository 500 m (Glacial)
Base Case

Glacial 3 advance	**pH**	**Eh (mV)**	**TDS**	**Ionic Strength**	**Alkalinity**	**C**	**Cl**	**S(6)**	**Ca**	**Mg**	**Na**	**K**	**Si**
Mean	8.82	−311.65	124.17	2.11E−03	8.27E−04	7.70E−04	7.05E−04	6.82E−05	3.34E−04	2.71E−05	9.42E−04	2.11E−05	1.48E−04
Standard Deviation	0.25	17.39	41.75	6.34E−04	4.09E−04	4.22E−04	2.94E−04	3.62E−05	1.01E−04	1.44E−05	4.64E−04	6.52E−06	7.42E−06
Minimum	8.10	−356.71	60.85	1.11E−03	2.37E−04	1.70E−04	3.89E−04	1.44E−05	2.34E−04	6.27E−06	2.25E−04	1.15E−05	1.37E−04
P0.1	8.10	−355.08	60.85	1.11E−03	2.37E−04	1.70E−04	3.89E−04	1.44E−05	2.34E−04	6.27E−06	2.25E−04	1.15E−05	1.37E−04
P5	8.40	−342.74	73.31	1.36E−03	2.93E−04	2.07E−04	4.39E−04	2.04E−05	2.44E−04	7.86E−06	3.42E−04	1.24E−05	1.40E−04
Median	8.81	−311.28	115.97	1.97E−03	7.56E−04	6.98E−04	6.13E−04	6.23E−05	3.00E−04	2.47E−05	8.60E−04	2.00E−05	1.46E−04
P95	9.26	−282.68	211.09	3.41E−03	1.56E−03	1.52E−03	1.20E−03	1.31E−04	5.06E−04	5.21E−05	1.79E−03	3.24E−05	1.64E−04
P99.9	9.42	−263.79	371.64	5.52E−03	3.24E−03	3.26E−03	3.35E−03	2.84E−04	1.27E−03	1.12E−04	3.74E−03	5.98E−05	1.77E−04
Maximum	9.43	−257.86	371.64	5.52E−03	3.24E−03	3.26E−03	3.35E−03	2.84E−04	1.27E−03	1.12E−04	3.74E−03	5.98E−05	1.77E−04
Glacial 4 advance	**pH**	**Eh (mV)**	**TDS**	**Ionic Strength**	**Alkalinity**	**C**	**Cl**	**S(6)**	**Ca**	**Mg**	**Na**	**K**	**Si**
Mean	8.78	−309.27	128.81	2.22E−03	8.11E−04	7.58E−04	8.07E−04	6.82E−05	3.67E−04	2.68E−05	9.62E−04	2.10E−05	1.47E−04
Standard Deviation	0.26	18.20	40.69	5.76E−04	4.05E−04	4.19E−04	1.62E−04	3.62E−05	5.55E−05	1.43E−05	4.64E−04	6.50E−06	7.61E−06
Minimum	8.05	−353.31	63.33	1.21E−03	2.26E−04	1.48E−04	5.55E−04	1.56E−05	2.88E−04	5.79E−06	2.63E−04	1.16E−05	1.37E−04
P0.1	8.05	−353.04	63.33	1.21E−03	2.26E−04	1.48E−04	5.55E−04	1.56E−05	2.88E−04	5.79E−06	2.63E−04	1.16E−05	1.37E−04
P5	8.39	−343.10	79.57	1.48E−03	2.75E−04	1.95E−04	5.88E−04	1.93E−05	2.90E−04	7.33E−06	3.56E−04	1.22E−05	1.40E−04
Median	8.75	−307.65	121.45	2.13E−03	7.50E−04	6.95E−04	7.88E−04	6.37E−05	3.57E−04	2.47E−05	8.88E−04	2.01E−05	1.45E−04
P95	9.27	−281.60	195.45	3.25E−03	1.53E−03	1.50E−03	1.10E−03	1.31E−04	4.67E−04	5.21E−05	1.75E−03	3.24E−05	1.65E−04
P99.9	9.37	−260.98	380.62	5.72E−03	3.22E−03	3.25E−03	1.48E−03	2.86E−04	5.94E−04	1.12E−04	3.79E−03	5.99E−05	1.73E−04
Maximum	9.37	−254.52	380.62	5.72E−03	3.22E−03	3.25E−03	1.48E−03	2.86E−04	5.94E−04	1.12E−04	3.79E−03	5.99E−05	1.73E−04
Glacial 5 advance	**pH**	**Eh (mV)**	**TDS**	**Ionic Strength**	**Alkalinity**	**C**	**Cl**	**S(6)**	**Ca**	**Mg**	**Na**	**K**	**Si**
Mean	8.84	−313.36	118.81	2.07E−03	7.33E−04	6.75E−04	7.70E−04	6.06E−05	3.55E−04	2.40E−05	8.58E−04	1.97E−05	1.49E−04
Standard Deviation	0.26	17.92	34.52	5.36E−04	3.24E−04	3.36E−04	2.51E−04	2.92E−05	8.49E−05	1.15E−05	3.79E−04	5.24E−06	8.38E−06
Minimum	8.25	−356.93	59.58	1.10E−03	2.36E−04	1.47E−04	4.17E−04	1.36E−05	2.41E−04	5.37E−06	2.23E−04	1.13E−05	1.38E−04
P0.1	8.26	−356.72	59.58	1.10E−03	2.36E−04	1.47E−04	4.17E−04	1.36E−05	2.41E−04	5.37E−06	2.23E−04	1.13E−05	1.38E−04
P5	8.46	−345.77	70.65	1.33E−03	2.73E−04	1.88E−04	4.70E−04	1.87E−05	2.53E−04	7.07E−06	3.15E−04	1.20E−05	1.40E−04
Median	8.81	−311.74	114.08	2.00E−03	6.95E−04	6.38E−04	7.26E−04	5.73E−05	3.38E−04	2.29E−05	8.23E−04	1.91E−05	1.46E−04
P95	9.30	−286.50	182.10	3.03E−03	1.28E−03	1.24E−03	1.20E−03	1.11E−04	5.02E−04	4.34E−05	1.53E−03	2.86E−05	1.67E−04
P99.9	9.43	−272.28	249.22	3.96E−03	1.94E−03	1.91E−03	1.86E−03	1.68E−04	7.30E−04	6.58E−05	2.28E−03	3.89E−05	1.77E−04
Maximum	9.43	−268.78	249.22	3.96E−03	1.94E−03	1.91E−03	1.86E−03	1.68E−04	7.30E−04	6.58E−05	2.28E−03	3.89E−05	1.77E−04
Glacial 5 retreat	**pH**	**Eh (mV)**	**TDS**	**Ionic Strength**	**Alkalinity**	**C**	**Cl**	**S(6)**	**Ca**	**Mg**	**Na**	**K**	**Si**
Mean	8.84	−313.36	118.81	2.07E−03	7.33E−04	6.75E−04	7.70E−04	6.06E−05	3.55E−04	2.40E−05	8.58E−04	1.97E−05	1.49E−04
Standard Deviation	0.26	17.92	34.52	5.36E−04	3.24E−04	3.36E−04	2.51E−04	2.92E−05	8.49E−05	1.15E−05	3.79E−04	5.24E−06	8.38E−06
Minimum	8.25	−356.93	59.58	1.10E−03	2.36E−04	1.47E−04	4.17E−04	1.36E−05	2.41E−04	5.37E−06	2.23E−04	1.13E−05	1.38E−04
P0.1	8.26	−356.72	59.58	1.10E−03	2.36E−04	1.47E−04	4.17E−04	1.36E−05	2.41E−04	5.37E−06	2.23E−04	1.13E−05	1.38E−04
P5	8.46	−345.77	70.65	1.33E−03	2.73E−04	1.88E−04	4.70E−04	1.87E−05	2.53E−04	7.07E−06	3.15E−04	1.20E−05	1.40E−04
Median	8.81	−311.74	114.08	2.00E−03	6.95E−04	6.38E−04	7.26E−04	5.73E−05	3.38E−04	2.29E−05	8.23E−04	1.91E−05	1.46E−04
P95	9.30	−286.50	182.10	3.03E−03	1.28E−03	1.24E−03	1.20E−03	1.11E−04	5.02E−04	4.34E−05	1.53E−03	2.86E−05	1.67E−04
P99.9	9.43	−272.28	249.22	3.96E−03	1.94E−03	1.91E−03	1.86E−03	1.68E−04	7.30E−04	6.58E−05	2.28E−03	3.89E−05	1.77E−04
Maximum	9.43	−268.78	249.22	3.96E−03	1.94E−03	1.91E−03	1.86E−03	1.68E−04	7.30E−04	6.58E−05	2.28E−03	3.89E−05	1.77E−04

Table A2-1. Continuation.

Repository 500 m (Glacial)
Base Case

Glacial 4 retreat	**pH**	**Eh (mV)**	**TDS**	**Ionic Strength**	**Alkalinity**	**C**	**Cl**	**S(6)**	**Ca**	**Mg**	**Na**	**K**	**Si**
Mean	8.91	−318.25	107.25	1.86E−03	6.69E−04	6.06E−04	6.82E−04	5.38E−05	3.25E−04	2.15E−05	7.54E−04	1.85E−05	1.51E−04
Standard Deviation	0.25	17.55	30.43	4.34E−04	2.93E−04	3.07E−04	9.97E−05	2.69E−05	3.34E−05	1.06E−05	3.49E−04	4.82E−06	9.78E−06
Minimum	8.29	−360.92	58.85	1.15E−03	2.48E−04	1.48E−04	5.48E−04	1.17E−05	2.88E−04	5.16E−06	1.91E−04	1.10E−05	1.38E−04
P0.1	8.29	−360.39	58.85	1.15E−03	2.48E−04	1.48E−04	5.48E−04	1.17E−05	2.88E−04	5.16E−06	1.91E−04	1.10E−05	1.38E−04
P5	8.55	−351.16	66.69	1.25E−03	2.75E−04	1.78E−04	5.59E−04	1.49E−05	2.88E−04	6.31E−06	2.55E−04	1.16E−05	1.41E−04
Median	8.89	−316.66	102.34	1.79E−03	6.35E−04	5.74E−04	6.42E−04	5.13E−05	3.12E−04	2.05E−05	7.19E−04	1.81E−05	1.48E−04
P95	9.40	−291.97	161.60	2.66E−03	1.18E−03	1.14E−03	8.25E−04	1.00E−04	3.74E−04	3.97E−05	1.35E−03	2.68E−05	1.75E−04
P99.9	9.48	−275.18	242.91	3.82E−03	1.92E−03	1.90E−03	9.90E−04	1.67E−04	4.29E−04	6.57E−05	2.24E−03	3.87E−05	1.83E−04
Maximum	9.49	−271.05	242.91	3.82E−03	1.92E−03	1.90E−03	9.90E−04	1.67E−04	4.29E−04	6.57E−05	2.24E−03	3.87E−05	1.83E−04

Glacial 2 retreat	**pH**	**Eh (mV)**	**TDS**	**Ionic Strength**	**Alkalinity**	**C**	**Cl**	**S(6)**	**Ca**	**Mg**	**Na**	**K**	**Si**
Mean	9.19	−337.05	73.44	1.26E−03	5.00E−04	4.14E−04	4.01E−04	3.38E−05	2.39E−04	1.44E−05	4.45E−04	1.51E−05	1.63E−04
Standard Deviation	0.20	14.69	18.85	2.70E−04	1.73E−04	1.88E−04	5.60E−05	1.71E−05	1.70E−05	6.70E−06	2.24E−04	3.06E−06	1.24E−05
Minimum	8.58	−366.23	45.67	7.99E−04	2.62E−04	1.52E−04	2.05E−04	9.42E−06	1.84E−04	4.81E−06	1.28E−04	1.07E−05	1.42E−04
P0.1	8.58	−366.20	45.67	7.99E−04	2.62E−04	1.52E−04	2.05E−04	9.42E−06	1.84E−04	4.81E−06	1.28E−04	1.07E−05	1.42E−04
P5	8.86	−361.25	50.35	9.43E−04	2.91E−04	1.74E−04	3.73E−04	1.10E−05	2.34E−04	5.41E−06	1.49E−04	1.10E−05	1.47E−04
Median	9.17	−336.01	71.39	1.24E−03	4.76E−04	3.93E−04	4.00E−04	3.22E−05	2.36E−04	1.38E−05	4.26E−04	1.48E−05	1.59E−04
P95	9.52	−313.01	108.61	1.77E−03	8.13E−04	7.48E−04	4.73E−04	6.37E−05	2.59E−04	2.61E−05	8.34E−04	2.05E−05	1.87E−04
P99.9	9.56	−296.39	158.84	2.55E−03	1.22E−03	1.17E−03	6.49E−04	1.02E−04	3.16E−04	4.07E−05	1.37E−03	2.72E−05	1.92E−04
Maximum	9.56	−290.96	158.84	2.55E−03	1.22E−03	1.17E−03	6.49E−04	1.02E−04	3.16E−04	4.07E−05	1.37E−03	2.72E−05	1.92E−04

Glacial 0 retreat	**pH**	**Eh (mV)**	**TDS**	**Ionic Strength**	**Alkalinity**	**C**	**Cl**	**S(6)**	**Ca**	**Mg**	**Na**	**K**	**Si**
Mean	8.05	−261.68	1215.27	2.86E−02	3.64E−04	3.44E−04	2.03E−02	1.76E−04	7.44E−03	1.55E−05	6.03E−03	2.70E−05	1.37E−04
Standard Deviation	0.24	16.67	129.59	3.24E−03	1.77E−04	1.89E−04	2.45E−03	1.33E−05	8.98E−04	6.51E−06	5.60E−04	2.24E−06	1.56E−06
Minimum	7.55	−300.97	898.29	2.05E−02	1.11E−04	7.48E−05	1.42E−02	1.36E−04	5.20E−03	6.42E−06	4.70E−03	2.22E−05	1.35E−04
P0.1	7.55	−300.93	898.29	2.05E−02	1.11E−04	7.48E−05	1.42E−02	1.36E−04	5.20E−03	6.42E−06	4.70E−03	2.22E−05	1.35E−04
P5	7.71	−292.09	1026.90	2.39E−02	1.25E−04	9.05E−05	1.68E−02	1.52E−04	6.16E−03	6.85E−06	5.16E−03	2.41E−05	1.36E−04
Median	7.99	−259.84	1202.45	2.82E−02	3.49E−04	3.27E−04	2.01E−02	1.76E−04	7.36E−03	1.49E−05	6.02E−03	2.66E−05	1.37E−04
P95	8.52	−237.07	1455.10	3.45E−02	6.77E−04	6.75E−04	2.48E−02	1.95E−04	9.08E−03	2.69E−05	7.04E−03	3.09E−05	1.41E−04
P99.9	8.59	−221.56	1529.10	3.64E−02	1.04E−03	1.07E−03	2.62E−02	2.18E−04	9.59E−03	4.12E−05	7.38E−03	3.66E−05	1.42E−04
Maximum	8.60	−221.39	1529.10	3.64E−02	1.04E−03	1.07E−03	2.62E−02	2.18E−04	9.59E−03	4.12E−05	7.38E−03	3.66E−05	1.42E−04

Table A2-2. Statistical results for the main geochemical parameters obtained with the geochemical Base Case over the glacial period when considering an ice-sheet advancing over a frozen ground (Permafrost) in the repository volume at 500 m depth. Chemical components in mol/kg, TDS in mg/L, pH in standard units and Eh in mV.

Repository 500 m (Permafrost)
Base Case

Permafrost 0 advance	**pH**	**Eh (mV)**	**TDS**	**Ionic Strength**	**Alkalinity**	**C**	**Ca**	**Mg**	**Na**	**K**	**Cl**	**S(6)**	**Si**
Mean	7.29	−208.54	893.27	1.65E−02	3.56E−03	3.96E−03	2.94E−03	1.48E−04	7.10E−03	8.06E−05	8.76E−03	4.30E−04	1.34E−04
Standard Deviation	0.08	12.36	138.03	3.21E−03	1.28E−04	6.85E−05	8.55E−04	1.09E−07	6.95E−04	1.38E−06	2.51E−03	1.73E−05	1.86E−07
Minimum	7.11	−227.93	693.37	1.19E−02	3.27E−03	3.80E−03	1.71E−03	1.48E−04	6.08E−03	7.86E−05	5.09E−03	4.05E−04	1.34E−04
P0.1	7.11	−227.80	693.37	1.19E−02	3.27E−03	3.80E−03	1.71E−03	1.48E−04	6.08E−03	7.86E−05	5.09E−03	4.05E−04	1.34E−04
P5	7.14	−224.42	723.01	1.25E−02	3.33E−03	3.83E−03	1.89E−03	1.48E−04	6.23E−03	7.89E−05	5.65E−03	4.09E−04	1.34E−04
Median	7.30	−210.00	860.99	1.57E−02	3.58E−03	3.97E−03	2.74E−03	1.48E−04	6.94E−03	8.03E−05	8.19E−03	4.26E−04	1.34E−04
P95	7.42	−183.35	1173.10	2.30E−02	3.75E−03	4.05E−03	4.68E−03	1.48E−04	8.50E−03	8.34E−05	1.38E−02	4.65E−04	1.34E−04
P99.9	7.45	−175.47	1268.00	2.53E−02	3.79E−03	4.07E−03	5.27E−03	1.48E−04	8.97E−03	8.43E−05	1.55E−02	4.77E−04	1.35E−04
Maximum	7.45	−174.25	1268.00	2.53E−02	3.79E−03	4.07E−03	5.27E−03	1.48E−04	8.97E−03	8.43E−05	1.55E−02	4.77E−04	1.35E−04

Permafrost 1 advance	**pH**	**Eh (mV)**	**TDS**	**Ionic Strength**	**Alkalinity**	**C**	**Ca**	**Mg**	**Na**	**K**	**Cl**	**S(6)**	**Si**
Mean	8.65	−301.22	147.90	2.14E−03	2.75E−03	6.73E−04	5.30E−04	2.43E−05	1.01E−03	2.01E−05	1.28E−03	6.52E−05	1.17E−07
Standard Deviation	0.27	18.01	55.13	8.73E−04	1.12E−03	1.99E−04	2.33E−04	7.11E−06	4.00E−04	3.56E−06	6.63E−04	2.21E−05	4.88E−09
Minimum	7.89	−332.32	83.35	1.11E−03	1.44E−03	3.71E−04	2.59E−04	1.35E−05	4.96E−04	1.49E−05	4.87E−04	3.37E−05	1.08E−07
P0.1	7.89	−332.01	83.35	1.11E−03	1.44E−03	3.71E−04	2.59E−04	1.35E−05	4.96E−04	1.49E−05	4.87E−04	3.37E−05	1.08E−07
P5	8.15	−326.53	88.66	1.21E−03	1.57E−03	4.39E−04	2.88E−04	1.60E−05	5.74E−04	1.61E−05	5.80E−04	4.04E−05	1.10E−07
Median	8.67	−302.28	136.61	1.97E−03	2.53E−03	6.22E−04	4.77E−04	2.26E−05	9.41E−04	1.93E−05	1.14E−03	6.01E−05	1.16E−07
P95	9.00	−269.30	264.50	4.04E−03	5.21E−03	1.03E−03	1.01E−03	3.71E−05	1.85E−03	2.68E−05	2.64E−03	1.09E−04	1.25E−07
P99.9	9.06	−247.68	373.90	5.79E−03	7.47E−03	1.48E−03	1.57E−03	5.31E−05	2.66E−03	3.47E−05	4.22E−03	1.56E−04	1.31E−07
Maximum	9.06	−245.47	373.90	5.79E−03	7.47E−03	1.48E−03	1.57E−03	5.31E−05	2.66E−03	3.47E−05	4.22E−03	1.56E−04	1.31E−07

Permafrost 2 advance	**pH**	**Eh (mV)**	**TDS**	**Ionic Strength**	**Alkalinity**	**C**	**Ca**	**Mg**	**Na**	**K**	**Cl**	**S(6)**	**Si**
Mean	8.89	−316.82	107.95	1.98E−03	5.54E−04	4.95E−04	3.91E−04	1.80E−05	6.95E−04	1.70E−05	8.81E−04	4.62E−05	1.49E−04
Standard Deviation	0.21	14.40	31.68	6.49E−04	9.73E−05	1.09E−04	1.37E−04	4.03E−06	2.31E−04	2.02E−06	4.01E−04	1.26E−05	5.88E−06
Minimum	8.23	−349.55	59.10	1.04E−03	3.93E−04	2.97E−04	2.19E−04	1.02E−05	2.93E−04	1.32E−05	3.31E−04	2.28E−05	1.38E−04
P0.1	8.23	−348.36	59.10	1.04E−03	3.93E−04	2.97E−04	2.19E−04	1.02E−05	2.93E−04	1.32E−05	3.31E−04	2.28E−05	1.38E−04
P5	8.48	−337.79	70.27	1.23E−03	4.32E−04	3.58E−04	2.37E−04	1.28E−05	4.09E−04	1.45E−05	4.07E−04	3.04E−05	1.41E−04
Median	8.90	−317.88	102.10	1.86E−03	5.30E−04	4.64E−04	3.63E−04	1.69E−05	6.54E−04	1.66E−05	8.10E−04	4.36E−05	1.48E−04
P95	9.19	−290.96	174.48	3.40E−03	7.21E−04	6.83E−04	6.75E−04	2.50E−05	1.17E−03	2.08E−05	1.70E−03	7.10E−05	1.60E−04
P99.9	9.32	−271.42	240.56	4.71E−03	9.82E−04	9.61E−04	9.94E−04	3.47E−05	1.67E−03	2.55E−05	2.60E−03	9.93E−05	1.69E−04
Maximum	9.33	−268.35	240.56	4.71E−03	9.82E−04	9.61E−04	9.94E−04	3.47E−05	1.67E−03	2.55E−05	2.60E−03	9.93E−05	1.69E−04

Table A2-2. Continuation.

Repository 500 m (Permafrost)
Base Case

Permafrost 3 advance	pH	Eh (mV)	TDS (mgL)	Ionic Strength	Alkalinity	C	Ca	Mg	Na	K	Cl	S(6)	Si
N total	1248	1248	624	624	6.24E+02	624	624	6.24E+02	624	6.24E+02	6.24E+02	624	624
Mean	9.34	−347.28	58.61	1.04E−03	3.79E−04	2.82E−04	2.29E−04	9.62E−06	2.78E−04	1.29E−05	3.55E−04	2.15E−05	1.70E−04
Standard Deviation	0.07	5.66	6.14	1.31E−04	2.02E−05	2.20E−05	2.96E−05	8.92E−07	4.81E−05	4.32E−07	1.03E−04	2.62E−06	5.01E−06
Minimum	9.04	−363.05	44.66	7.69E−04	3.36E−04	2.31E−04	1.85E−04	7.06E−06	1.46E−04	1.17E−05	1.68E−04	1.37E−05	1.53E−04
P0.1	9.05	−362.72	44.66	7.69E−04	3.36E−04	2.31E−04	1.85E−04	7.06E−06	1.46E−04	1.17E−05	1.68E−04	1.37E−05	1.53E−04
P5	9.24	−356.42	49.06	8.45E−04	3.45E−04	2.52E−04	1.91E−04	8.26E−06	1.99E−04	1.22E−05	2.06E−04	1.72E−05	1.63E−04
Median	9.34	−347.42	58.05	1.03E−03	3.80E−04	2.80E−04	2.22E−04	9.56E−06	2.78E−04	1.29E−05	3.37E−04	2.13E−05	1.70E−04
P95	9.45	−338.93	68.77	1.26E−03	4.15E−04	3.24E−04	2.83E−04	1.12E−05	3.54E−04	1.37E−05	5.33E−04	2.60E−05	1.79E−04
P99.9	9.52	−324.14	89.67	1.71E−03	4.42E−04	3.52E−04	3.76E−04	1.30E−05	5.05E−04	1.47E−05	8.38E−04	3.29E−05	1.87E−04
Maximum	9.52	−323.58	89.67	1.71E−03	4.42E−04	3.52E−04	3.76E−04	1.30E−05	5.05E−04	1.47E−05	8.38E−04	3.29E−05	1.87E−04

Permafrost 4 advance	pH	Eh (mV)	TDS (mgL)	Ionic Strength	Alkalinity	C	Ca	Mg	Na	K	Cl	S(6)	Si
N total	1248	1248	624	624	6.24E+02	624	624	6.24E+02	624	6.24E+02	6.24E+02	624	624
Mean	9.04	−327.95	107.63	2.21E−03	3.07E−04	2.45E−04	1.29E−03	2.81E−05	5.33E−04	9.67E−06	5.40E−04	1.35E−05	1.54E−04
Standard Deviation	0.07	6.15	12.77	2.98E−04	2.18E−05	2.39E−05	2.20E−04	2.97E−06	7.60E−05	8.91E−07	7.28E−05	4.47E−07	3.02E−06
Minimum	8.79	−346.43	78.99	1.57E−03	2.63E−04	1.86E−04	8.44E−04	1.91E−05	3.87E−04	7.11E−06	3.52E−04	1.21E−05	1.46E−04
P0.1	8.79	−346.35	78.99	1.57E−03	2.63E−04	1.86E−04	8.44E−04	1.91E−05	3.87E−04	7.11E−06	3.52E−04	1.21E−05	1.46E−04
P5	8.93	−338.56	86.40	1.73E−03	2.78E−04	2.13E−04	9.56E−04	2.27E−05	4.23E−04	8.30E−06	4.08E−04	1.27E−05	1.49E−04
Median	9.04	−328.30	107.05	2.20E−03	3.03E−04	2.42E−04	1.28E−03	2.83E−05	5.28E−04	9.61E−06	5.44E−04	1.35E−05	1.53E−04
P95	9.19	−318.75	130.96	2.76E−03	3.49E−04	2.89E−04	1.66E−03	3.26E−05	6.63E−04	1.12E−05	6.59E−04	1.42E−05	1.60E−04
P99.9	9.27	−308.56	151.91	3.25E−03	3.89E−04	3.36E−04	2.07E−03	3.94E−05	8.06E−04	1.30E−05	8.12E−04	1.52E−05	1.65E−04
Maximum	9.27	−306.83	151.91	3.25E−03	3.89E−04	3.36E−04	2.07E−03	3.94E−05	8.06E−04	1.30E−05	8.12E−04	1.52E−05	1.65E−04

Table A2-3. Statistical results for the main geochemical parameters obtained with the geochemical Base Case over the glacial period when considering an ice-sheet advancing over unfrozen ground in the repository volume at 700 m depth. Chemical components in mol/kg, TDS in mg/L, pH in standard units and Eh in mV.

Repository 700 m (Glacial)
Base Case

Glacial 0 advance	**pH**	**Eh (mV)**	**TDS**	**Ionic Strength**	**Alkalinity**	**C**	**Cl**	**S(6)**	**Ca**	**Mg**	**Na**	**K**	**Si**
Mean	6.72	−143.19	9713.22	2.26E−01	2.43E−03	3.14E−03	1.63E−01	1.49E−03	5.88E−02	1.41E−04	4.98E−02	1.66E−04	1.27E−04
Standard Deviation	0.22	49.29	6359.66	1.52E−01	4.81E−04	4.10E−04	1.11E−01	7.62E−04	4.04E−02	4.80E−06	3.07E−02	6.10E−05	5.25E−06
Minimum	6.52	−225.84	723.74	1.26E−02	1.95E−03	2.64E−03	5.66E−03	4.09E−04	1.89E−03	1.34E−04	6.24E−03	7.89E−05	1.19E−04
P0.1	6.52	−225.84	723.74	1.26E−02	1.95E−03	2.64E−03	5.66E−03	4.09E−04	1.89E−03	1.34E−04	6.24E−03	7.89E−05	1.19E−04
P5	6.53	−208.02	1135.90	2.22E−02	1.97E−03	2.67E−03	1.32E−02	4.60E−04	4.44E−03	1.35E−04	8.32E−03	8.30E−05	1.20E−04
Median	6.62	−171.38	9814.85	2.29E−01	2.24E−03	3.04E−03	1.65E−01	1.50E−03	5.95E−02	1.41E−04	5.04E−02	1.67E−04	1.26E−04
P95	7.16	−71.74	18380.00	4.33E−01	3.35E−03	3.84E−03	3.14E−01	2.53E−03	1.14E−01	1.48E−04	9.17E−02	2.49E−04	1.34E−04
P99.9	7.42	−70.83	19026.00	4.48E−01	3.74E−03	4.05E−03	3.25E−01	2.60E−03	1.18E−01	1.48E−04	9.48E−02	2.55E−04	1.34E−04
Maximum	7.42	−70.83	19026.00	4.48E−01	3.74E−03	4.05E−03	3.25E−01	2.60E−03	1.18E−01	1.48E−04	9.48E−02	2.55E−04	1.34E−04
Glacial 1 advance	**pH**	**Eh (mV)**	**TDS**	**Ionic Strength**	**Alkalinity**	**C**	**Cl**	**S(6)**	**Ca**	**Mg**	**Na**	**K**	**Si**
Mean	8.05	−257.27	2146.14	5.03E−02	6.07E−04	6.24E−04	3.60E−02	3.14E−04	1.31E−02	2.70E−05	1.08E−02	4.12E−05	1.39E−04
Standard Deviation	0.76	58.53	2455.03	5.80E−02	3.44E−04	4.29E−04	4.19E−02	3.39E−04	1.52E−02	1.95E−05	1.23E−02	3.23E−05	8.23E−06
Minimum	6.85	−346.78	105.71	2.04E−03	1.72E−04	1.15E−04	7.74E−04	1.87E−05	3.52E−04	5.42E−06	4.44E−04	1.17E−05	1.29E−04
P0.1	6.85	−346.78	105.71	2.04E−03	1.72E−04	1.15E−04	7.74E−04	1.87E−05	3.52E−04	5.42E−06	4.44E−04	1.17E−05	1.29E−04
P5	6.99	−328.76	116.72	2.34E−03	1.82E−04	1.36E−04	1.28E−03	2.84E−05	5.25E−04	6.45E−06	6.00E−04	1.29E−05	1.29E−04
Median	8.21	−270.64	623.40	1.44E−02	5.25E−04	4.85E−04	1.01E−02	1.04E−04	3.71E−03	1.87E−05	3.15E−03	2.33E−05	1.38E−04
P95	9.05	−147.34	6896.10	1.63E−01	1.19E−03	1.36E−03	1.17E−01	9.76E−04	4.26E−02	6.11E−05	3.44E−02	1.04E−04	1.54E−04
P99.9	9.28	−121.86	7264.20	1.71E−01	1.57E−03	1.93E−03	1.24E−01	1.00E−03	4.50E−02	8.60E−05	3.62E−02	1.12E−04	1.66E−04
Maximum	9.28	−121.86	7264.20	1.71E−01	1.57E−03	1.93E−03	1.24E−01	1.00E−03	4.50E−02	8.60E−05	3.62E−02	1.12E−04	1.66E−04
Glacial 2 advance	**pH**	**Eh (mV)**	**TDS**	**Ionic Strength**	**Alkalinity**	**C**	**Cl**	**S(6)**	**Ca**	**Mg**	**Na**	**K**	**Si**
Mean	8.73	−307.01	796.55	1.86E−02	3.46E−04	2.91E−04	1.31E−02	1.17E−04	4.85E−03	1.22E−05	3.92E−03	2.14E−05	1.56E−04
Standard Deviation	0.77	52.03	1114.01	2.64E−02	1.61E−04	1.97E−04	1.90E−02	1.54E−04	6.90E−03	8.94E−06	5.57E−03	1.48E−05	1.78E−05
Minimum	7.20	−363.50	57.83	1.14E−03	1.64E−04	1.11E−04	5.47E−04	1.03E−05	2.88E−04	4.46E−06	1.71E−04	1.08E−05	1.32E−04
P0.1	7.20	−363.50	57.83	1.14E−03	1.64E−04	1.11E−04	5.47E−04	1.03E−05	2.88E−04	4.46E−06	1.71E−04	1.08E−05	1.32E−04
P5	7.41	−358.22	61.02	1.18E−03	1.81E−04	1.19E−04	5.52E−04	1.21E−05	2.90E−04	4.63E−06	2.13E−04	1.09E−05	1.34E−04
Median	9.14	−336.05	110.79	2.39E−03	2.79E−04	2.12E−04	1.51E−03	2.53E−05	6.19E−04	7.80E−06	5.48E−04	1.31E−05	1.58E−04
P95	9.47	−219.08	3187.60	7.51E−02	6.84E−04	7.08E−04	5.39E−02	4.50E−04	1.97E−02	3.12E−05	1.59E−02	5.33E−05	1.82E−04
P99.9	9.52	−179.08	4456.90	1.05E−01	8.78E−04	9.51E−04	7.55E−02	6.29E−04	2.75E−02	4.22E−05	2.23E−02	7.06E−05	1.87E−04
Maximum	9.52	−179.08	4456.90	1.05E−01	8.78E−04	9.51E−04	7.55E−02	6.29E−04	2.75E−02	4.22E−05	2.23E−02	7.06E−05	1.87E−04

Table A2-3. Continuation.

Repository 700 m (Glacial)
Base Case

Glacial 3 advance	pH	Eh (mV)	TDS	Ionic Strength	Alkalinity	C	Cl	S(6)	Ca	Mg	Na	K	Si
Mean	8.80	−311.80	610.19	1.42E−02	3.09E−04	2.50E−04	9.98E−03	9.09E−05	3.70E−03	1.05E−05	2.99E−03	1.88E−05	1.56E−04
Standard Deviation	0.68	45.46	840.72	1.99E−02	1.22E−04	1.47E−04	1.44E−02	1.16E−04	5.21E−03	6.64E−06	4.20E−03	1.10E−05	1.65E−05
Minimum	7.35	−360.52	59.36	1.16E−03	1.63E−04	1.10E−04	5.49E−04	1.15E−05	2.89E−04	4.47E−06	2.00E−04	1.09E−05	1.33E−04
P0.1	7.35	−360.52	59.36	1.16E−03	1.63E−04	1.10E−04	5.49E−04	1.15E−05	2.89E−04	4.47E−06	2.00E−04	1.09E−05	1.33E−04
P5	7.58	−356.38	61.17	1.18E−03	1.82E−04	1.16E−04	5.52E−04	1.24E−05	2.90E−04	4.64E−06	2.28E−04	1.10E−05	1.35E−04
Median	9.18	−335.94	104.44	2.26E−03	2.72E−04	1.87E−04	1.42E−03	2.39E−05	5.94E−04	7.72E−06	5.39E−04	1.28E−05	1.60E−04
P95	9.45	−228.35	2414.70	5.69E−02	5.82E−04	5.57E−04	4.07E−02	3.42E−04	1.49E−02	2.46E−05	1.20E−02	4.28E−05	1.80E−04
P99.9	9.48	−202.01	3446.50	8.12E−02	7.27E−04	7.61E−04	5.83E−02	4.87E−04	2.13E−02	3.35E−05	1.72E−02	5.68E−05	1.82E−04
Maximum	9.48	−202.01	3446.50	8.12E−02	7.27E−04	7.61E−04	5.83E−02	4.87E−04	2.13E−02	3.35E−05	1.72E−02	5.68E−05	1.82E−04

Glacial 4 advance	pH	Eh (mV)	TDS	Ionic Strength	Alkalinity	C	Cl	S(6)	Ca	Mg	Na	K	Si
Mean	8.99	−324.11	231.07	5.25E−03	2.08E−04	1.52E−04	3.58E−03	3.72E−05	1.36E−03	6.93E−06	1.09E−03	1.35E−05	1.53E−04
Standard Deviation	0.21	14.60	131.58	3.16E−03	6.49E−05	6.55E−05	2.31E−03	1.71E−05	8.32E−04	2.25E−06	6.47E−04	1.66E−06	7.25E−06
Minimum	8.49	−351.46	104.10	1.99E−03	1.48E−04	9.38E−05	9.30E−04	1.65E−05	4.04E−04	4.58E−06	4.16E−04	1.13E−05	1.41E−04
P0.1	8.49	−351.46	104.10	1.99E−03	1.48E−04	9.38E−05	9.30E−04	1.65E−05	4.04E−04	4.58E−06	4.16E−04	1.13E−05	1.41E−04
P5	8.62	−343.47	106.34	2.27E−03	1.59E−04	9.76E−05	1.42E−03	1.92E−05	5.83E−04	4.72E−06	4.55E−04	1.17E−05	1.43E−04
Median	9.03	−326.38	178.33	3.94E−03	1.88E−04	1.35E−04	2.64E−03	3.04E−05	1.03E−03	6.35E−06	8.26E−04	1.29E−05	1.53E−04
P95	9.27	−296.65	517.86	1.21E−02	3.09E−04	2.52E−04	8.57E−03	7.37E−05	3.16E−03	1.01E−05	2.50E−03	1.69E−05	1.66E−04
P99.9	9.35	−286.42	620.54	1.46E−02	5.59E−04	5.06E−04	1.03E−02	8.81E−05	3.80E−03	1.85E−05	3.02E−03	1.81E−05	1.71E−04
Maximum	9.35	−286.42	620.54	1.46E−02	5.59E−04	5.06E−04	1.03E−02	8.81E−05	3.80E−03	1.85E−05	3.02E−03	1.81E−05	1.71E−04

Glacial 5 advance	pH	Eh (mV)	TDS	Ionic Strength	Alkalinity	C	Cl	S(6)	Ca	Mg	Na	K	Si
Mean	9.00	−324.59	219.72	4.98E−03	1.97E−04	1.42E−04	3.40E−03	3.52E−05	1.29E−03	6.64E−06	1.03E−03	1.33E−05	1.53E−04
Standard Deviation	0.13	9.53	67.66	1.64E−03	6.42E−05	6.63E−05	1.22E−03	8.68E−06	4.39E−04	2.25E−06	3.24E−04	1.05E−06	4.43E−06
Minimum	8.55	−346.23	125.59	2.43E−03	1.41E−04	8.50E−05	1.26E−03	2.05E−05	5.18E−04	4.66E−06	5.75E−04	1.16E−05	1.42E−04
P0.1	8.55	−346.23	125.59	2.43E−03	1.41E−04	8.50E−05	1.26E−03	2.05E−05	5.18E−04	4.66E−06	5.75E−04	1.16E−05	1.42E−04
P5	8.76	−337.98	135.49	2.97E−03	1.47E−04	8.86E−05	1.86E−03	2.41E−05	7.34E−04	4.78E−06	6.30E−04	1.22E−05	1.45E−04
Median	9.02	−326.06	215.48	4.91E−03	1.75E−04	1.24E−04	3.37E−03	3.40E−05	1.28E−03	5.98E−06	1.02E−03	1.30E−05	1.53E−04
P95	9.16	−305.47	365.58	8.49E−03	2.99E−04	2.47E−04	5.97E−03	5.33E−05	2.22E−03	1.01E−05	1.74E−03	1.51E−05	1.59E−04
P99.9	9.27	−291.15	393.20	9.14E−03	5.47E−04	4.99E−04	6.43E−03	5.68E−05	2.39E−03	1.85E−05	1.88E−03	1.75E−05	1.65E−04
Maximum	9.27	−291.15	393.20	9.14E−03	5.47E−04	4.99E−04	6.43E−03	5.68E−05	2.39E−03	1.85E−05	1.88E−03	1.75E−05	1.65E−04

Glacial 5 retreat	pH	Eh (mV)	TDS	Ionic Strength	Alkalinity	C	Cl	S(6)	Ca	Mg	Na	K	Si
Mean	9.00	−324.59	219.72	4.98E−03	1.97E−04	1.42E−04	3.40E−03	3.52E−05	1.29E−03	6.64E−06	1.03E−03	1.33E−05	1.53E−04
Standard Deviation	0.13	9.53	67.66	1.64E−03	6.42E−05	6.63E−05	1.22E−03	8.68E−06	4.39E−04	2.25E−06	3.24E−04	1.05E−06	4.43E−06
Minimum	8.55	−346.23	125.59	2.43E−03	1.41E−04	8.50E−05	1.26E−03	2.05E−05	5.18E−04	4.66E−06	5.75E−04	1.16E−05	1.42E−04
P0.1	8.55	−346.23	125.59	2.43E−03	1.41E−04	8.50E−05	1.26E−03	2.05E−05	5.18E−04	4.66E−06	5.75E−04	1.16E−05	1.42E−04
P5	8.76	−337.98	135.49	2.97E−03	1.47E−04	8.86E−05	1.86E−03	2.41E−05	7.34E−04	4.78E−06	6.30E−04	1.22E−05	1.45E−04
Median	9.02	−326.06	215.48	4.91E−03	1.75E−04	1.24E−04	3.37E−03	3.40E−05	1.28E−03	5.98E−06	1.02E−03	1.30E−05	1.53E−04
P95	9.16	−305.47	365.58	8.49E−03	2.99E−04	2.47E−04	5.97E−03	5.33E−05	2.22E−03	1.01E−05	1.74E−03	1.51E−05	1.59E−04
P99.9	9.27	−291.15	393.20	9.14E−03	5.47E−04	4.99E−04	6.43E−03	5.68E−05	2.39E−03	1.85E−05	1.88E−03	1.75E−05	1.65E−04
Maximum	9.27	−291.15	393.20	9.14E−03	5.47E−04	4.99E−04	6.43E−03	5.68E−05	2.39E−03	1.85E−05	1.88E−03	1.75E−05	1.65E−04

Table A2-3. Continuation.

Repository 700 m (Glacial)
Base Case

Glacial 4 retreat	pH	Eh (mV)	TDS	Ionic Strength	Alkalinity	C	Cl	S(6)	Ca	Mg	Na	K	Si
Mean	9.29	−344.22	114.80	2.49E−03	2.08E−04	1.30E−04	1.59E−03	1.92E−05	6.54E−04	5.34E−06	4.83E−04	1.17E−05	1.67E−04
Standard Deviation	0.10	7.48	33.47	8.09E−04	3.65E−05	3.57E−05	6.10E−04	4.79E−06	2.14E−04	1.24E−06	1.67E−04	6.03E−07	6.28E−06
Minimum	9.04	−359.33	75.37	1.56E−03	1.65E−04	1.00E−04	7.40E−04	1.20E−05	3.44E−04	4.33E−06	2.60E−04	1.09E−05	1.54E−04
P0.1	9.04	−359.33	75.37	1.56E−03	1.65E−04	1.00E−04	7.40E−04	1.20E−05	3.44E−04	4.33E−06	2.60E−04	1.09E−05	1.54E−04
P5	9.08	−354.72	80.27	1.60E−03	1.68E−04	1.04E−04	8.99E−04	1.38E−05	4.10E−04	4.38E−06	3.14E−04	1.11E−05	1.55E−04
Median	9.31	−345.36	107.04	2.29E−03	2.02E−04	1.21E−04	1.42E−03	1.80E−05	5.97E−04	4.99E−06	4.53E−04	1.15E−05	1.68E−04
P95	9.41	−329.82	183.15	4.14E−03	2.63E−04	1.82E−04	2.81E−03	3.03E−05	1.09E−03	7.03E−06	8.24E−04	1.28E−05	1.76E−04
P99.9	9.46	−323.92	223.32	5.10E−03	4.07E−04	3.39E−04	3.51E−03	3.33E−05	1.33E−03	1.25E−05	1.03E−03	1.45E−05	1.81E−04
Maximum	9.46	−323.92	223.32	5.10E−03	4.07E−04	3.39E−04	3.51E−03	3.33E−05	1.33E−03	1.25E−05	1.03E−03	1.45E−05	1.81E−04
Glacial 2 retreat	**pH**	**Eh (mV)**	**TDS**	**Ionic Strength**	**Alkalinity**	**C**	**Cl**	**S(6)**	**Ca**	**Mg**	**Na**	**K**	**Si**
Mean	9.50	−359.11	65.27	1.32E−03	2.53E−04	1.42E−04	6.85E−04	1.11E−05	3.57E−04	4.61E−06	2.08E−04	1.08E−05	1.86E−04
Standard Deviation	0.08	6.77	19.63	4.71E−04	3.26E−05	2.08E−05	3.75E−04	3.01E−06	1.22E−04	5.64E−07	1.06E−04	3.38E−07	8.71E−06
Minimum	9.30	−368.85	48.52	9.28E−04	1.93E−04	1.14E−04	3.71E−04	7.86E−06	2.40E−04	4.19E−06	1.07E−04	1.05E−05	1.68E−04
P0.1	9.30	−368.85	48.52	9.28E−04	1.93E−04	1.14E−04	3.71E−04	7.86E−06	2.40E−04	4.19E−06	1.07E−04	1.05E−05	1.68E−04
P5	9.34	−368.33	48.60	9.29E−04	1.99E−04	1.16E−04	3.71E−04	7.99E−06	2.53E−04	4.20E−06	1.09E−04	1.05E−05	1.70E−04
Median	9.53	−360.69	57.33	1.14E−03	2.56E−04	1.40E−04	5.46E−04	1.01E−05	3.12E−04	4.53E−06	1.63E−04	1.07E−05	1.89E−04
P95	9.59	−346.83	104.19	2.25E−03	2.90E−04	1.70E−04	1.42E−03	1.79E−05	5.98E−04	5.23E−06	4.18E−04	1.14E−05	1.96E−04
P99.9	9.60	−342.03	114.04	2.49E−03	3.44E−04	2.45E−04	1.59E−03	1.83E−05	6.58E−04	8.31E−06	4.71E−04	1.23E−05	1.96E−04
Maximum	9.60	−342.03	114.04	2.49E−03	3.44E−04	2.45E−04	1.59E−03	1.83E−05	6.58E−04	8.31E−06	4.71E−04	1.23E−05	1.96E−04
Glacial 0 retreat	**pH**	**Eh (mV)**	**TDS**	**Ionic Strength**	**Alkalinity**	**C**	**Cl**	**S(6)**	**Ca**	**Mg**	**Na**	**K**	**Si**
Mean	8.60	−296.49	1 760.20	4.19E−02	1.06E−04	6.89E−05	3.02E−02	2.22E−04	1.11E−02	6.47E−06	8.50E−03	2.85E−05	1.42E−04
Standard Deviation	0.09	7.76	379.70	9.08E−03	1.41E−05	1.53E−05	6.58E−03	4.69E−05	2.40E−03	6.60E−07	1.85E−03	3.93E−06	1.36E−06
Minimum	8.16	−310.02	944.50	2.24E−02	9.48E−05	5.76E−05	1.61E−02	1.22E−04	5.90E−03	5.66E−06	4.53E−03	2.02E−05	1.37E−04
P0.1	8.16	−310.02	944.50	2.24E−02	9.48E−05	5.76E−05	1.61E−02	1.22E−04	5.90E−03	5.66E−06	4.53E−03	2.02E−05	1.37E−04
P5	8.48	−307.10	1 044.90	2.48E−02	9.58E−05	5.80E−05	1.78E−02	1.34E−04	6.54E−03	5.79E−06	5.02E−03	2.11E−05	1.40E−04
Median	8.61	−296.92	1 850.55	4.41E−02	1.03E−04	6.64E−05	3.18E−02	2.33E−04	1.16E−02	6.38E−06	8.93E−03	2.97E−05	1.42E−04
P95	8.70	−285.34	2 264.40	5.40E−02	1.19E−04	8.47E−05	3.90E−02	2.85E−04	1.42E−02	7.21E−06	1.10E−02	3.38E−05	1.44E−04
P99.9	8.74	−263.28	2 475.40	5.90E−02	1.98E−04	1.70E−04	4.26E−02	3.10E−04	1.56E−02	1.01E−05	1.20E−02	3.58E−05	1.45E−04
Maximum	8.74	−263.28	2 475.40	5.90E−02	1.98E−04	1.70E−04	4.26E−02	3.10E−04	1.56E−02	1.01E−05	1.20E−02	3.58E−05	1.45E−04

Table A2-4. Statistical results for the main geochemical parameters obtained with the geochemical Base Case over the glacial period when considering an ice-sheet advancing over a frozen ground (Permafrost) in the repository volume at 700 m depth. Chemical components in mol/kg, TDS in mg/L, pH in standard units and Eh in mV.

Repository 700 m (Permafrost)
Base Case

Permafrost 0 advance	pH	Eh (mV)	TDS	Ionic Strength	Alkalinity	C	Cl	S(6)	Ca	Mg	Na	K	Si
Mean	6.96	−172.65	2213.87	4.76E−02	2.98E−03	3.62E−03	3.22E−02	5.91E−04	1.12E−02	1.47E−04	1.36E−02	9.35E−05	1.33E−04
Standard Deviation	0.12	30.01	886.34	2.10E−02	2.32E−04	1.40E−04	1.56E−02	1.07E−04	5.60E−03	6.76E−07	4.32E−03	8.58E−06	7.96E−07
Minimum	6.77	−215.07	957.41	1.80E−02	2.59E−03	3.38E−03	9.94E−03	4.38E−04	3.33E−03	1.45E−04	7.42E−03	8.12E−05	1.31E−04
P0.1	6.77	−215.07	957.41	1.80E−02	2.59E−03	3.38E−03	9.94E−03	4.38E−04	3.33E−03	1.45E−04	7.42E−03	8.12E−05	1.31E−04
P5	6.78	−208.93	1134.80	2.21E−02	2.61E−03	3.39E−03	1.31E−02	4.60E−04	4.44E−03	1.45E−04	8.31E−03	8.30E−05	1.31E−04
Median	6.96	−186.43	1980.45	4.21E−02	2.98E−03	3.63E−03	2.82E−02	5.63E−04	9.75E−03	1.47E−04	1.25E−02	9.13E−05	1.33E−04
P95	7.16	−116.29	4098.80	9.24E−02	3.35E−03	3.84E−03	6.53E−02	8.18E−04	2.32E−02	1.48E−04	2.28E−02	1.12E−04	1.34E−04
P99.9	7.24	−112.62	4217.40	9.52E−02	3.49E−03	3.92E−03	6.73E−02	8.33E−04	2.39E−02	1.48E−04	2.33E−02	1.13E−04	1.34E−04
Maximum	7.24	−112.62	4217.40	9.52E−02	3.49E−03	3.92E−03	6.73E−02	8.33E−04	2.39E−02	1.48E−04	2.33E−02	1.13E−04	1.34E−04

Permafrost 1 advance	pH	Eh (mV)	TDS	Ionic Strength	Alkalinity	C	Cl	S(6)	Ca	Mg	Na	K	Si
Mean	7.80	−245.20	609.32	1.32E−02	1.12E−03	1.14E−03	8.50E−03	1.62E−04	3.11E−03	4.26E−05	3.62E−03	3.26E−05	1.36E−04
Standard Deviation	0.23	17.00	290.65	6.68E−03	2.78E−04	3.18E−04	4.76E−03	5.61E−05	1.71E−03	1.20E−05	1.57E−03	7.32E−06	8.77E−07
Minimum	7.25	−273.61	269.22	5.13E−03	6.34E−04	6.19E−04	2.60E−03	9.43E−05	9.94E−04	2.40E−05	1.86E−03	2.25E−05	1.34E−04
P0.1	7.25	−273.61	269.22	5.13E−03	6.34E−04	6.19E−04	2.60E−03	9.43E−05	9.94E−04	2.40E−05	1.86E−03	2.25E−05	1.34E−04
P5	7.32	−267.37	308.33	6.33E−03	6.91E−04	6.81E−04	3.72E−03	1.03E−04	1.40E−03	2.59E−05	1.95E−03	2.42E−05	1.35E−04
Median	7.85	−248.25	512.16	1.10E−02	1.13E−03	1.14E−03	7.16E−03	1.40E−04	2.63E−03	4.13E−05	3.03E−03	3.07E−05	1.37E−04
P95	8.12	−213.44	1295.40	2.89E−02	1.67E−03	1.82E−03	1.95E−02	2.94E−04	7.00E−03	7.00E−05	7.27E−03	5.02E−05	1.38E−04
P99.9	8.14	−191.78	1402.50	3.09E−02	1.78E−03	1.97E−03	2.09E−02	3.34E−04	7.57E−03	7.64E−05	8.16E−03	5.50E−05	1.38E−04
Maximum	8.14	−191.78	1402.50	3.09E−02	1.78E−03	1.97E−03	2.09E−02	3.34E−04	7.57E−03	7.64E−05	8.16E−03	5.50E−05	1.38E−04

Permafrost 2 advance	pH	Eh (mV)	TDS	Ionic Strength	Alkalinity	C	Cl	S(6)	Ca	Mg	Na	K	Si
Mean	8.11	−266.17	415.71	8.97E−03	7.95E−04	7.85E−04	5.74E−03	1.09E−04	2.13E−03	2.95E−05	2.42E−03	2.50E−05	1.38E−04
Standard Deviation	0.30	20.84	245.64	5.58E−03	2.64E−04	2.94E−04	3.90E−03	5.11E−05	1.40E−03	1.09E−05	1.37E−03	6.77E−06	1.66E−06
Minimum	7.37	−303.01	161.60	3.23E−03	4.30E−04	4.00E−04	1.72E−03	5.54E−05	6.81E−04	1.61E−05	9.86E−04	1.78E−05	1.35E−04
P0.1	7.37	−303.01	161.60	3.23E−03	4.30E−04	4.00E−04	1.72E−03	5.54E−05	6.81E−04	1.61E−05	9.86E−04	1.78E−05	1.35E−04
P5	7.45	−291.57	183.97	3.50E−03	4.78E−04	4.52E−04	2.00E−03	6.00E−05	7.79E−04	1.75E−05	1.17E−03	1.82E−05	1.35E−04
Median	8.23	−271.64	317.69	6.95E−03	7.46E−04	7.23E−04	4.36E−03	8.83E−05	1.63E−03	2.70E−05	1.83E−03	2.30E−05	1.39E−04
P95	8.48	−228.08	995.85	2.19E−02	1.39E−03	1.47E−03	1.50E−02	2.42E−04	5.49E−03	5.57E−05	5.81E−03	4.24E−05	1.41E−04
P99.9	8.60	−206.33	1157.40	2.55E−02	1.54E−03	1.66E−03	1.71E−02	2.75E−04	6.19E−03	6.35E−05	6.70E−03	4.70E−05	1.42E−04
Maximum	8.60	−206.33	1157.40	2.55E−02	1.54E−03	1.66E−03	1.71E−02	2.75E−04	6.19E−03	6.35E−05	6.70E−03	4.70E−05	1.42E−04

Table A2-4. Continuation.

Repository 700 m (Permafrost)
Base Case

Permafrost 3 advance	**pH**	**Eh (mV)**	**TDS (mgL)**	**Ionic Strength**	**Alkalinity**	**C**	**Cl**	**S(6)**	**Ca**	**Mg**	**Na**	**K**	**Si**
N total	192	192	96	96	96	96	96	96	96	96	96	96	96
Mean	8.79	−310.86	225.22	4.82E−03	4.75E−04	4.24E−04	3.03E−03	5.63E−05	1.16E−03	1.60E−05	1.23E−03	1.74E−05	1.53E−04
Standard Deviation	0.59	39.02	231.24	5.18E−03	2.78E−04	3.14E−04	3.53E−03	5.36E−05	1.26E−03	1.18E−05	1.35E−03	7.29E−06	1.23E−05
Minimum	7.48	−352.20	61.46	1.15E−03	2.47E−04	1.78E−04	4.84E−04	1.74E−05	2.64E−04	6.83E−06	2.65E−04	1.20E−05	1.35E−04
P0.1	7.48	−352.20	61.46	1.15E−03	2.47E−04	1.78E−04	4.84E−04	1.74E−05	2.64E−04	6.83E−06	2.65E−04	1.20E−05	1.35E−04
P5	7.61	−347.43	65.16	1.22E−03	2.73E−04	1.96E−04	5.25E−04	1.86E−05	2.84E−04	7.47E−06	2.82E−04	1.22E−05	1.36E−04
Median	9.13	−331.77	95.88	1.96E−03	3.50E−04	2.71E−04	1.12E−03	2.54E−05	4.79E−04	9.89E−06	4.62E−04	1.34E−05	1.57E−04
P95	9.33	−236.34	809.89	1.79E−02	1.15E−03	1.18E−03	1.19E−02	1.90E−04	4.35E−03	4.45E−05	4.63E−03	3.54E−05	1.69E−04
P99.9	9.36	−216.01	977.06	2.16E−02	1.35E−03	1.43E−03	1.44E−02	2.32E−04	5.23E−03	5.40E−05	5.63E−03	4.11E−05	1.71E−04
Maximum	9.36	−216.01	977.06	2.16E−02	1.35E−03	1.43E−03	1.44E−02	2.32E−04	5.23E−03	5.40E−05	5.63E−03	4.11E−05	1.71E−04
Permafrost 4 advance	**pH**	**Eh (mV)**	**TDS (mgL)**	**Ionic Strength**	**Alkalinity**	**C**	**Cl**	**S(6)**	**Ca**	**Mg**	**Na**	**K**	**Si**
N total	192	192	96	96	96	96	96	96	96	96	96	96	96
Mean	8.67	−303.62	226.49	4.97E−03	3.46E−04	3.05E−04	3.26E−03	4.88E−05	1.23E−03	1.24E−05	1.18E−03	1.59E−05	1.45E−04
Standard Deviation	0.25	17.28	68.13	1.55E−03	1.29E−04	1.37E−04	1.07E−03	1.69E−05	3.86E−04	4.82E−06	3.94E−04	2.53E−06	4.34E−06
Minimum	8.22	−330.91	135.82	2.85E−03	1.95E−04	1.47E−04	1.74E−03	2.80E−05	6.89E−04	7.00E−06	6.57E−04	1.29E−05	1.39E−04
P0.1	8.22	−330.91	135.82	2.85E−03	1.95E−04	1.47E−04	1.74E−03	2.80E−05	6.89E−04	7.00E−06	6.57E−04	1.29E−05	1.39E−04
P5	8.29	−323.28	139.35	3.01E−03	2.12E−04	1.65E−04	1.93E−03	3.10E−05	7.61E−04	7.58E−06	7.04E−04	1.33E−05	1.39E−04
Median	8.80	−310.69	214.81	4.71E−03	2.87E−04	2.39E−04	3.05E−03	3.90E−05	1.16E−03	9.97E−06	1.04E−03	1.43E−05	1.46E−04
P95	8.97	−274.59	375.50	8.50E−03	5.64E−04	5.31E−04	5.78E−03	7.64E−05	2.15E−03	2.02E−05	1.94E−03	2.00E−05	1.51E−04
P99.9	9.03	−268.61	416.53	9.38E−03	7.33E−04	7.07E−04	6.34E−03	8.33E−05	2.35E−03	2.62E−05	2.20E−03	2.19E−05	1.53E−04
Maximum	9.03	−268.61	416.53	9.38E−03	7.33E−04	7.07E−04	6.34E−03	8.33E−05	2.35E−03	2.62E−05	2.20E−03	2.19E−05	1.53E−04

Appendix 3

Other geochemical components

This chapter includes a series of plots with the statistical results for the major components (and some interesting minor components) mentioned in Chapter 3. Their evolution over the whole glacial cycle is shown in Figures A3-1 to A3-4. The results correspond to the simulation of the Base Case over the grid points included in the repository volume at the two depths studied here, namely 500 and 700 m.

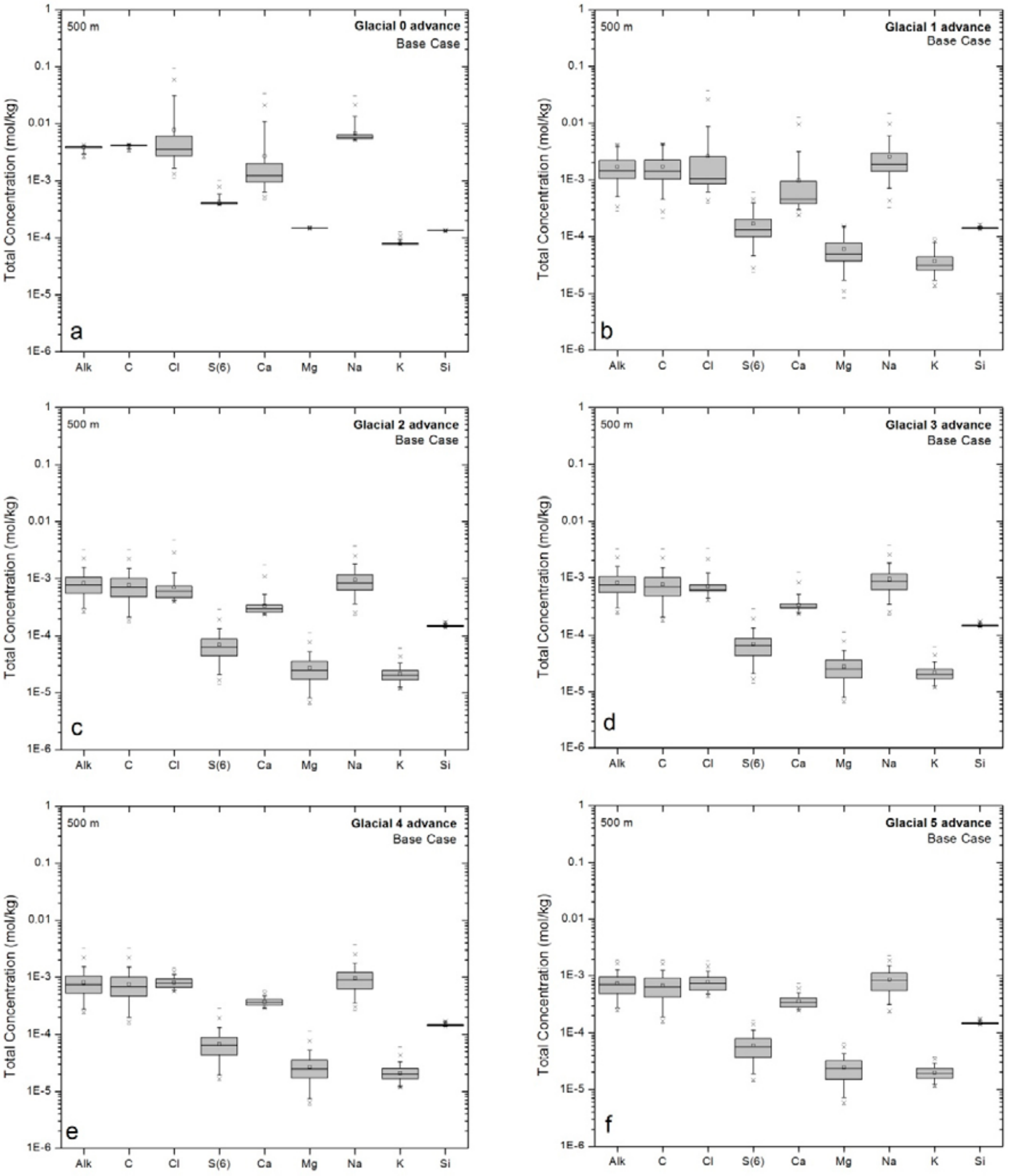

Figure A3-1. *Box-and-whisker plots showing the statistical distribution of the total concentration for the different major water components (in mol/kg) calculated with the Base Case over the advance stages of the Glacial period when considering an ice-sheet advancing over unfrozen ground (panels a to f) for the groundwater located within the SE-SFL repository volume at 500 m at Laxemar. The statistical measures plotted here and in all the following box and whisker plots, are the median (horizontal line inside the grey box), the 25th and 75th percentiles (bottom and top of the box), the mean (square), the 5th and 95th percentiles ("whiskers"), the 1st and 99th percentile (crosses) and the maximum and the minimum values (horizontal bars).*

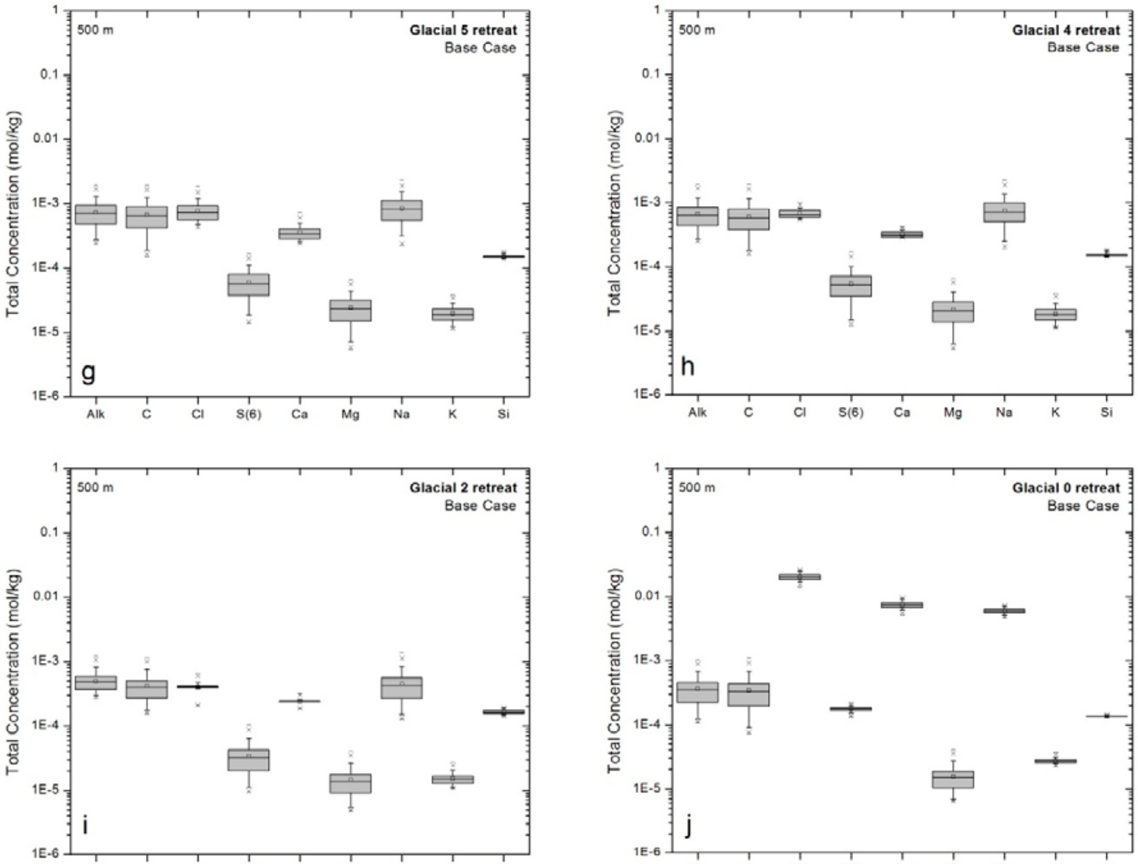

Figure A3-1. ***Cont.*** *Box-and-whisker plots showing the statistical distribution of the total concentration for the different major water components (in mol/kg) calculated with the Base Case over the retreat stages of the Glacial period (panels g to j) for the groundwater located within the SE-SFL repository volume at 500 m depth in Laxemar.*

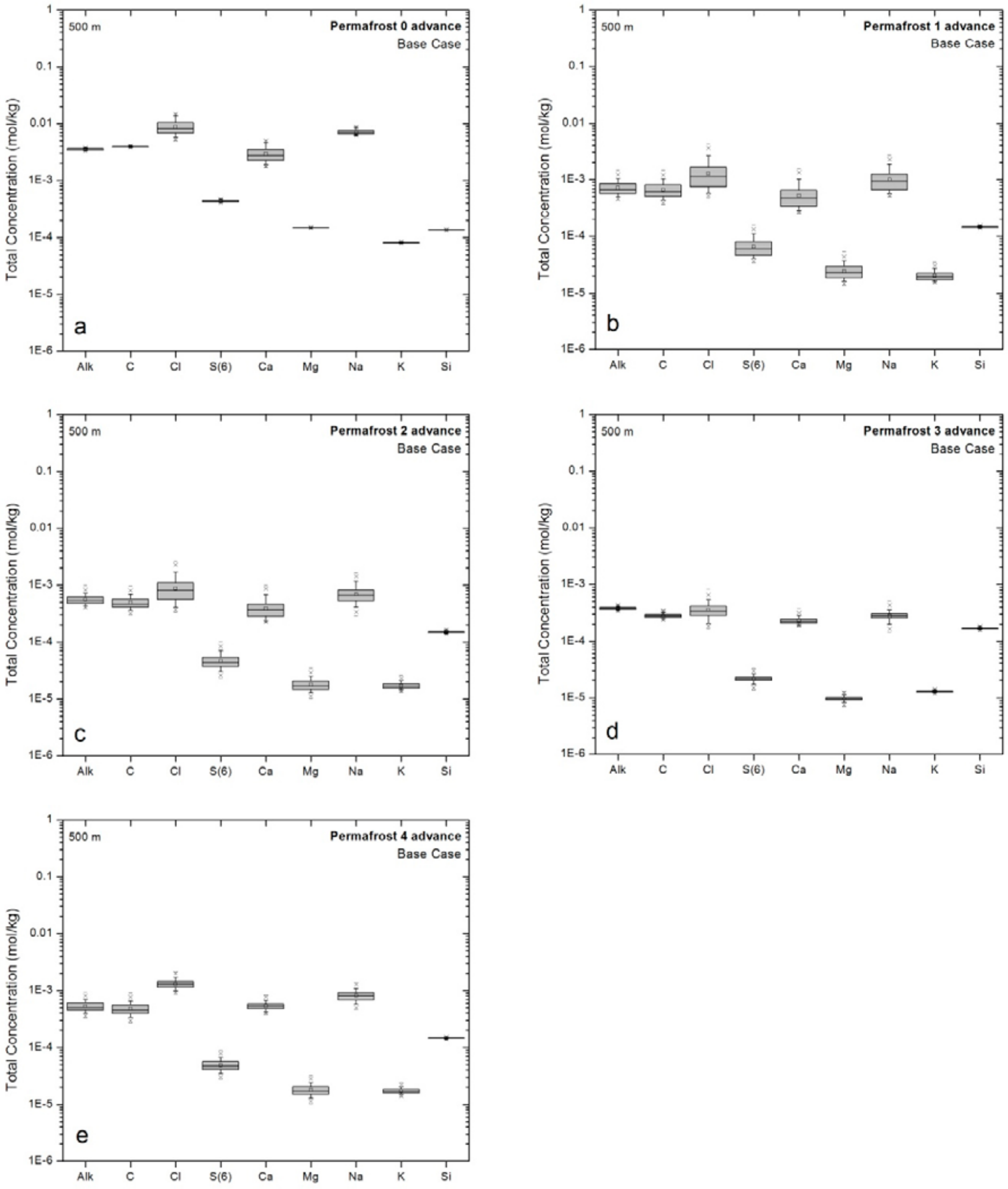

Figure A3-2. Box-and-whisker plots showing the statistical distribution of the total concentration for the different major water components (in mol/kg) calculated with the Base Case over the first stages of the Glacial period when considering an ice-sheet advancing over a frozen ground (permafrost) for the groundwater located within the SE-SFL repository volume at 500 m depth in Laxemar. The statistical values are the same as indicated in Figure A3-1 caption.

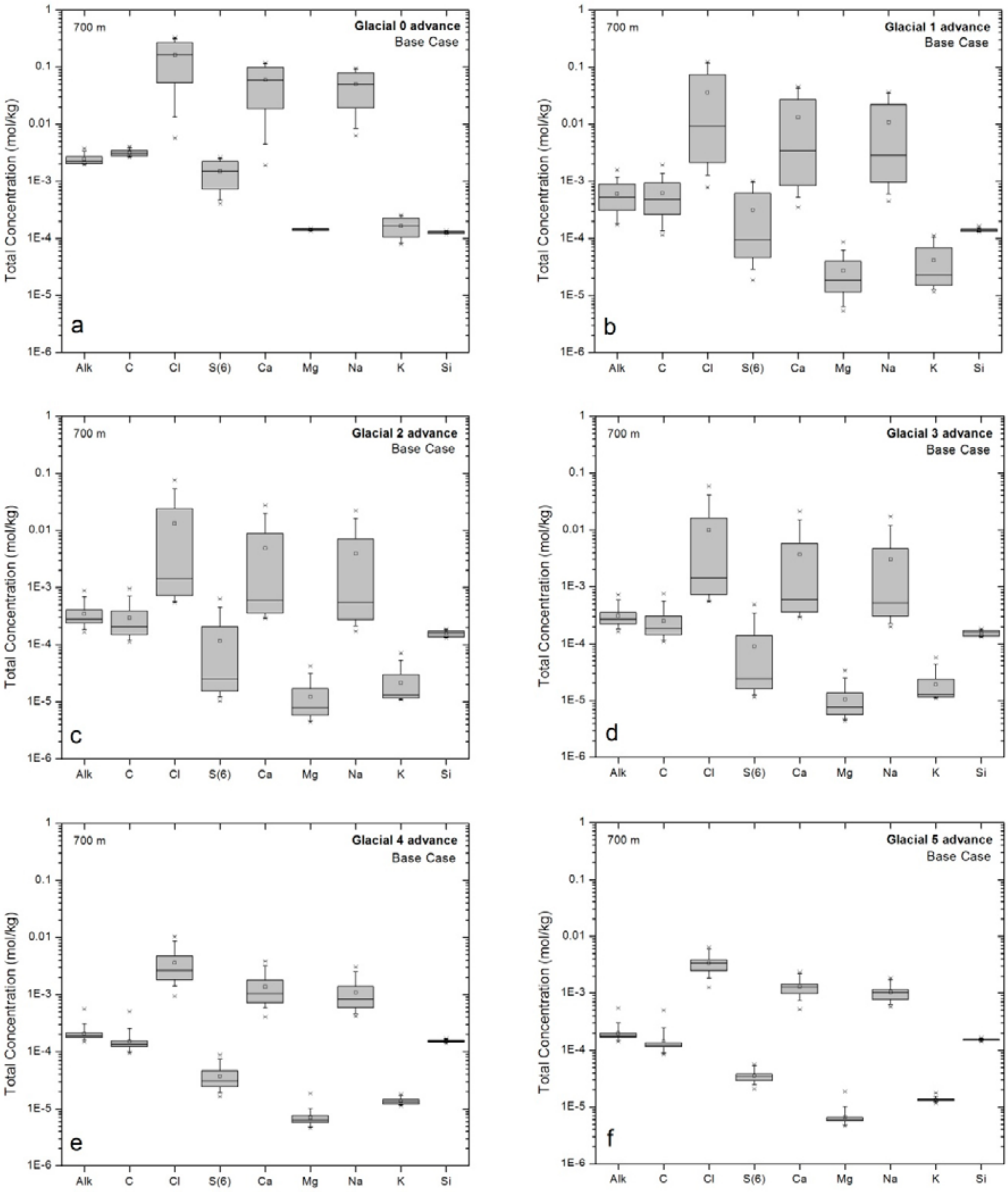

Figure A3-3. *Box-and-whisker plots showing the statistical distribution of the total concentration for the different major water components (in mol/kg) calculated with the Base Case over the advance stages of the Glacial period (panels a to f), when considering an ice-sheet advancing over unfrozen ground, for the groundwater located within the SE-SFL repository volume at 700 m at Laxemar. The statistical values are the same as indicated in Figure A3-1 caption.*

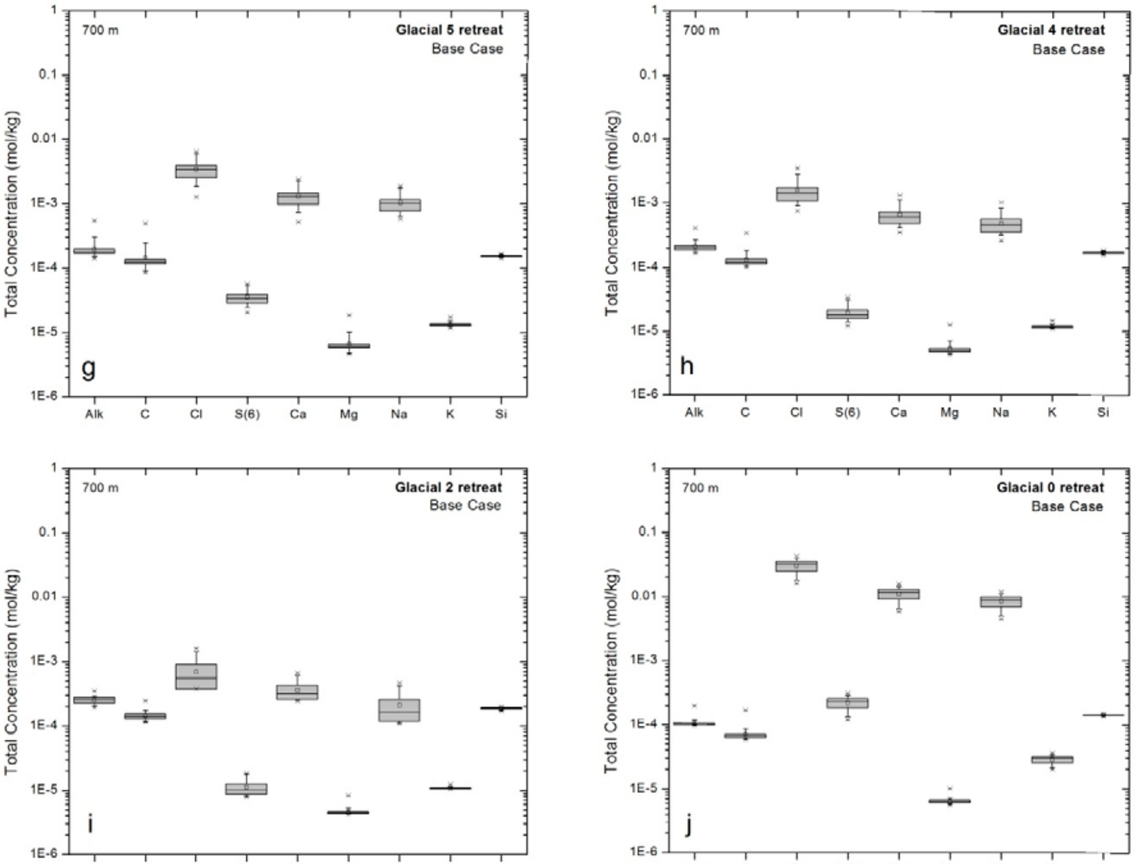

Figure A3-3. *Cont. Box-and-whisker plots showing the statistical distribution of the total concentration for the different major water components (in mol/kg) calculated with the Base Case over the retreat stages of the Glacial period (panels g to j) for the groundwater located within the SE-SFL repository volume at Laxemar. The statistical values are the same as indicated in Figure A3-1 caption.*

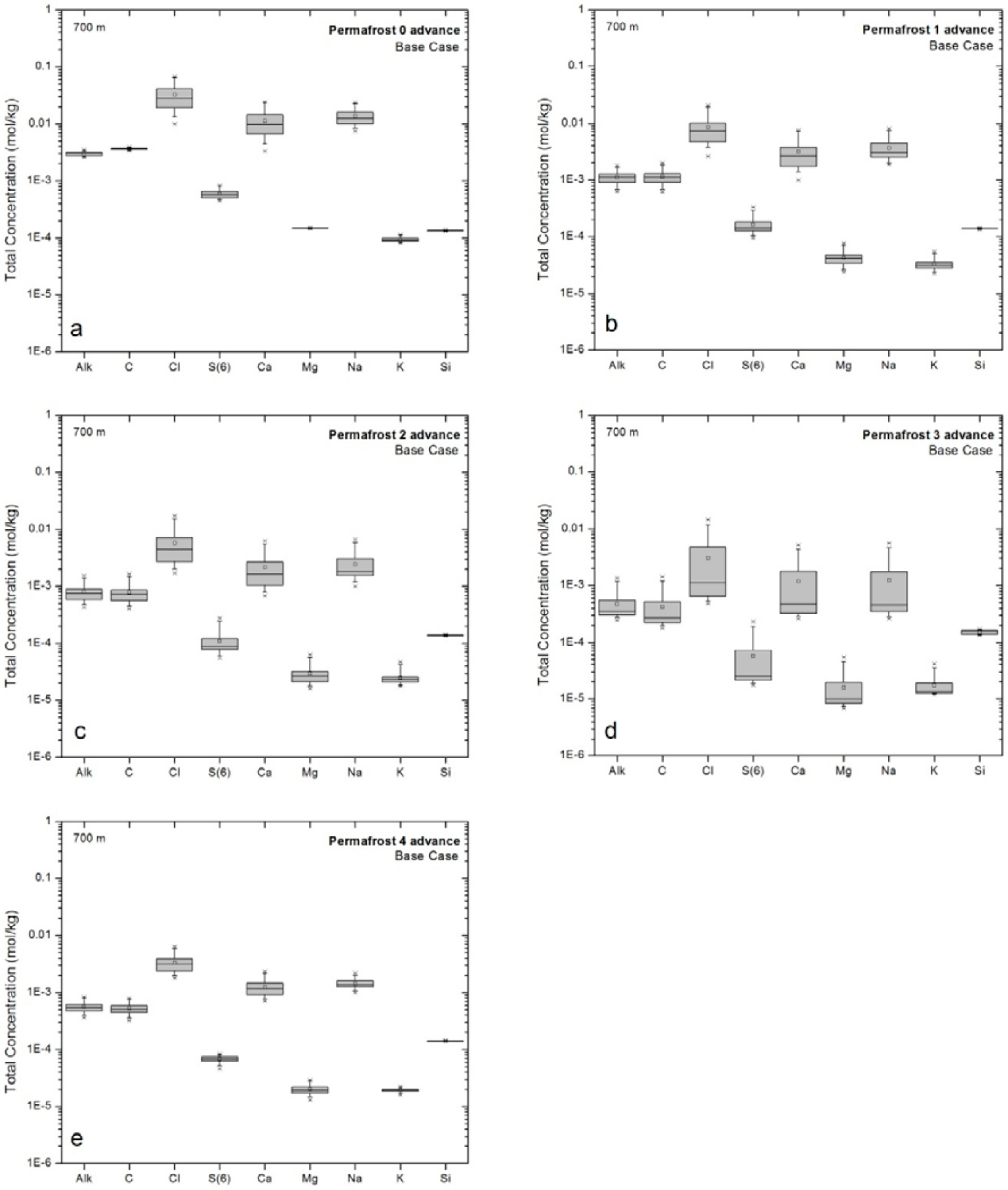

***Figure A3-4.** Box-and-whisker plots showing the statistical distribution of the total concentration for the different major water components (in mol/kg) calculated with the Base Case over the first stages of the Glacial period when considering an ice-sheet advancing over a frozen ground (permafrost) for the groundwater located within the SE-SFL repository volume at 700 m in Laxemar. The statistical values are the same as indicated in Figure A3-1 caption.*

Arkitektkopia AB, Bromma, 2019

SKB is responsible for managing spent nuclear fuel and radioactive waste produced by the Swedish nuclear power plants such that man and the environment are protected in the near and distant future.

skb.se

SVENSK KÄRNBRÄNSLEHANTERING